THE NLRP3 INFLAMMASOME CONTRIBUTES TO STATIN MYOPATHY

INVESTIGATING THE ROLE OF THE NLRP3 INFLAMMASOME IN STATIN-INDUCED MYOPATHY

by YUJIN LI, BSc.

A Thesis Submitted to the School of Graduate Studies in Partial Fulfilment if the Requirements for the Degree of Master of Science

McMaster University MASTER OF SCIENCE (2016) Hamilton, Ontario (Medical Sciences)

TITLE: Investigating the role of the NLRP3 inflammasome in statin-induced myopathy
AUTHOR: Yujin Li, BSc. (McMaster University)
SUPERVISOR: Dr. Jonathan D. Schertzer
NUMBER OF PAGES: xiii, 77

LAY ABSTRACT

Statins are a class of widely prescribed cholesterol-lowering drugs that reduce the risk of heart attack and stroke. However, many patients often complain of statin-induced muscle side effects (myopathy) that impact their quality of life. Symptoms of this statin-induced myopathy can manifest as muscle pain and weakness. The underlying biology causing this condition is still not well understood. Independent of its cholesterol-lowering effect, statins can activate an immune receptor called the NLRP3 inflammasome, indicating that inflammation may contribute to myopathy. Therefore, the primary goal of this study was to determine if this immune response contributes to statin-induced myopathy. It was found that inhibition of the NLRP3 inflammasome lowers markers of statin myopathy. Results from this study will provide further insight into mechanisms regulating this myopathy, and may lead to new treatments that can help alleviate statin side effects in muscle.

ABSTRACT

As a front-line treatment for cardiovascular disease, statins are among some of the most widely prescribed drugs worldwide. Statins are effective at lowering cholesterol, but approximately 7-29% of patients report some form of adverse muscle effect during the course of treatment. The severity of these side effects ranges from low-level to life-threatening myopathy. The mechanism of statin myopathy remains ill-defined, but muscle-specific E3 ubiquitin ligases have been implicated. In addition, statins have been shown to activate caspase-1 (and increase IL-1β) in immune cells, which is a key effector of the NLRP3 inflammasome. The relevance of this inflammatory response in statin myopathy remains unknown.

Using C2C12 myotubes, an *in vitro* model of statin-induced myopathy was developed to test the impact of NLRP3 inflammasome activation on markers of statin myopathy. Gene expression of the muscle-specific E3 ubiquitin ligases atrogin-1 and MuRF-1 (atrogenes) were used as markers of statin-induced myopathy. Lipopolysaccharide priming of the NLRP3 inflammasome was found to lower the effective dose of fluvastatin required to augment atrogene expression. This effect correlated with reduced phosphorylation of Akt and FOXO3a, a transcription factor regulating atrogene expression. Statin-induced atrogene expression was also found to be dependent on an isoprenoid that is required for protein prenylation rather than cholesterol biosynthesis pathways. Fluvastatin increased caspase-1 activity in a prenylation-dependent manner

and selective inhibitors of NLRP3 and caspase-1 were able to prevent increased atrogene expression with fluvastatin treatment.

Therefore, the NLRP3 inflammasome contributes to markers of statin-induced myopathy through a prenylation-dependant pathway in muscle cells. This work presents a novel mechanism involved in statin myopathy, and has shown that the inflammasome may represent a new drug target to mitigate muscle symptoms in patients taking statins.

ACKNOWLEDGEMENTS

I would like to thank and acknowledge the numerous individuals who have helped and contributed to this project. First and foremost, I would like to thank my supervisor, Dr. Jonathan Schertzer, without whom this research project would not have been possible. Thank you Jon for your amazing mentorship and your willingness to teach along the way. I don't think I would have been as excited for this project if not for the enthusiasm and genuine interest you had in this work. Your work ethic and passion for what you do are what I aspire to attain in my own future career.

A special thank you to Dr. Kevin Foley for his wisdom and constant supply of humor. I would also like to acknowledge all of my fellow lab mates in the Schertzer lab, who have made my time here so memorable. I am also grateful to Irena Rebalka from Dr. Hawke's lab for always being open to answering muscle questions and providing invaluable advice.

Finally, I would like to thank my family and friends who have supported me throughout my graduate studies. I would not have gotten here without the love and encouragement I have received along the way.

TABLE OF CONTENTS

LIST OF FIGURES

LIST OF TABLES

LIST OF ABBREVIATIONS

4EBP	4E binding protein
AFC	7-amino-4-trifluoromethylcoumarin
AIM	Absent in melanoma 2
ALR	AIM-like receptor
ANOVA	Analysis of variance
ARC	Apoptosis repressor with caspase recruitment domain
ASC	Apoptosis-associated speck-like protein containing a carboxy-terminal CARD
BCA	Bicinchoninic assay
Bcl-2	B-cell lymphoma 2
BSA	Bovine serum albumin
CARD	Caspase recruitment domain
cDNA	Complimentary deoxynucleic acid
CK	Creatine kinase
CoQ10	Coenzyme Q10
DAMP	Danger-associated molecular patterns
DMEM	Dulbecco's modified Eagle medium
DMSO	Dimethyl sulfoxide
DNA	Deoxyribonucleic acid
DTT	Dithiothreitol
eIF4E	Eukaryotic translation initiation factor 4E
FBS	Fetal bovine serum
FLICA	Fluorescent inhibitor of caspases
FOXO	Forkhead box gene group O
FPP	Farnesyl pyrophosphate
GAPDH	Glyceraldehyde 3-phosphate dehydrogenase
GGPP	Geranylgeranyl pyrophosphate
GSK3β	Glycogen synthase kinase 3 beta
HMG-CoA	3-hydroxy-3-methylglutaryl coenzyme A
HMGR	HMG-CoA reductase
IGF1	Insulin-like growth factor 1
IL-1	Interleukin-1
IL-18	Interleukin-18
IL-6	Interleukin-6

IRS	Insulin receptor substrate
LDL	Low-density lipoprotein
LPS	Lipopolysaccharide
MAFbx	Muscle atrophy F-box
mTOR	Mechanistic target of rapamycin
mTORC1	mTOR complex 1
mTORC2	mTOR complex 2
MuRF-1	Muscle RING-finger protein-1
NLR	Nucleotide-binding domain, leucine-rich repeat
NLRP3	Nucleotide-binding domain, leucine-rich repeat containing protein, pyrin domain-containing-3
NOD	Nucleotide-binding oligomerization domain-containing protein
OATP	Organic anion transport protein
pAkt	Phosphorylated Akt
PAMP	Pathogen-associated molecular patterns
PBS	Phosphate-buffered saline
PDK1	3-phosphoinositide-dependent protein kinase 1
PI3K	Phosphoinositide 3-kinase
PIP3	Phosphatidylinositol (3,4,5)-trisphosphate
PVDF	Polyvinylidene fluoride
RNA	Ribonucleic acid
ROS	Reactive oxygen species
RPLP0	Ribosomal protein, large, P0
RT-qPCR	Reverse transcription quantitative polymerase chain reaction
S6K	S6 kinase
SD	Standard deviation
SDS-PAGE	Sodium dodecyl sulfate polyacrylamide gel electrophoresis
SEM	Standard error of the mean
Ser	Serine
TBS	Tris-buffered saline
Thr	Threonine
TLR4	Toll-like receptor 4
TNFα	Tumor necrosis factor alpha

DECLARATION OF ACADEMIC ACHIEVEMENT

The following is a declaration that the content of the research presented in this thesis have been completed by Yujin Li, with some assistance from Jane McBride and Trevor Lau with sample preparation. This research study was designed by Dr. Jonathan Schertzer, who also contributed to the review and completion of this thesis. To the best of my knowledge, the content of this thesis does not infringe on the copyright of any others.

1.0 INTRODUCTION

In the early 1970s in their search for cholesterol-lowering compounds for use in cardiovascular disease, Endo and Kuroda identified a product from mold they called mevastatin[1]. Subsequently it was found that this statin compound inhibited the rate-limiting enzyme in cholesterol biosynthesis, 3-hydroxy-3-methylglutaryl coenzyme A reductase (HMGR)[2]. Mevastatin competes with the natural substrate, HMG-CoA for HMGR and consequently inhibits endogenous cholesterol synthesis. Since the initial identification of mevastatin, a number of natural and synthetic strategies have been used to develop more potent statins that have even greater affinity and prolonged binding to HMGR. Nearly a dozen statins have been developed and they now constitute one of the most commonly prescribed class of medications worldwide, having become established therapies for the primary and secondary prevention of cardiovascular disease[3,4]. Examples of popular statins on the market include fluvastatin (Lescol), atorvastatin (Lipitor), rosuvastatin (Crestor), lovastatin (Mevacor), and pravastatin (Pravacol)[5]. Although all statins have the same primary mechanism of action, statins can differ in their pharmacokinetics and pharmacodynamics. For example, pravastatin is extremely hydrophilic compared to other statins, which can impart significant clinical differences in patient susceptibility to statin effects.

In addition to the inhibition of endogenous cholesterol production, statin inhibition of HMGR also increases the level of low-density lipoprotein (LDL) receptors on

hepatocytes, resulting in a greater clearance of cholesterol from the circulation[6]. Statins have also been shown to inhibit the secretion of lipoproteins, and inhibit LDL oxidation, which represent additional factors that may reduce plaque formation to improve cardiovascular health[7]. These multiple modes of action largely account for the potent cholesterol-lowering ability of statins, and together are responsible for lowering patient risk of cardiovascular morbidity and mortality[4,8].

1.1 THE MEVALONATE PATHWAY

HMGR catalyzes the rate-limiting step in the mevalonate pathway, an important metabolic pathway that provides cells with essential bioactive molecules that are vital for many cellular processes[9]. A proximal step in this pathway is the conversion of HMG-CoA to mevalonate by HMGR. In subsequent steps, mevalonate is then converted into sterol isoprenoids, such as cholesterol, bile acids, lipoproteins, and steroid hormones, and a number of non-sterol isoprenoids, like ubiquinone, dolichol pyrophosphate, and the farnesyl and geranylgeranyl moieties of isoprenylated proteins (Figure 1). Non-sterol isoprenoids and intermediates in the mevalonate pathway contribute to post-translational modification of a multitude of proteins involved in cell growth and proliferation, intracellular signaling, gene expression, protein glycosylation, and cytoskeletal assembly[6].

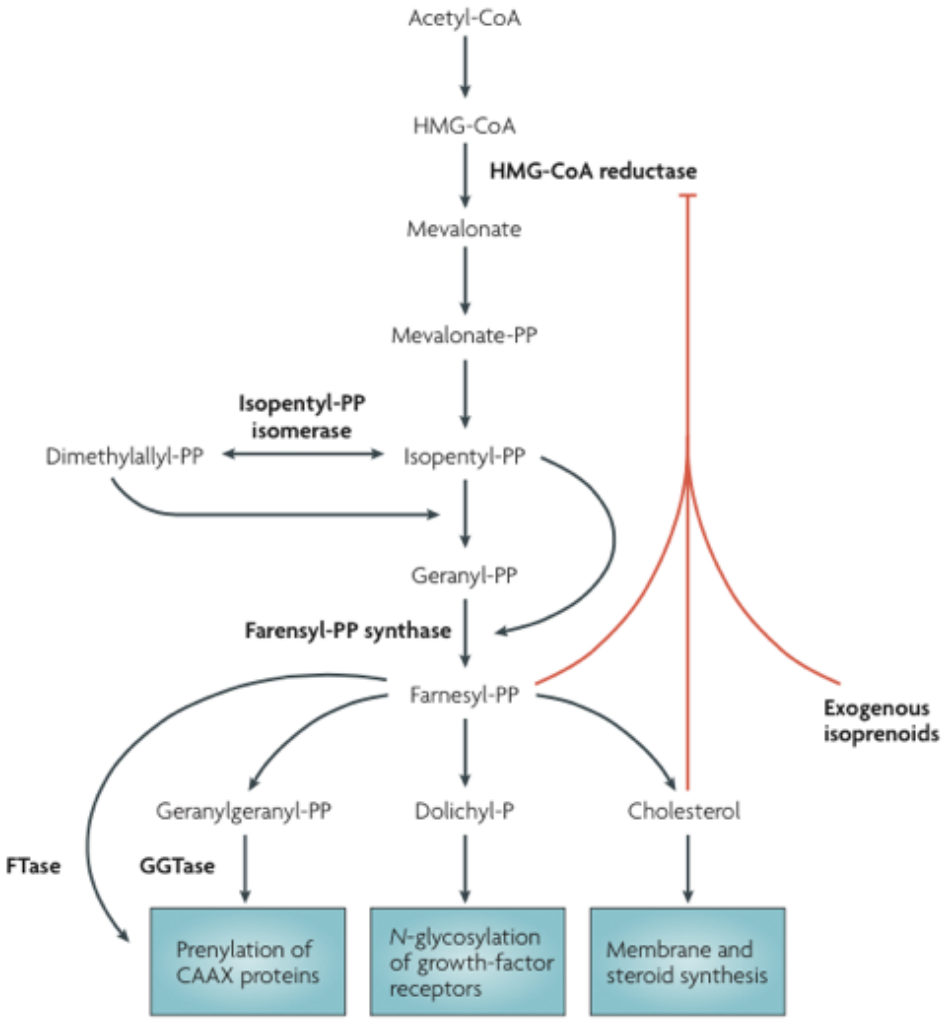

Figure 1| The mevalonate pathway.

3-hydroxy 3-methylglutaryl-CoA (HMG-CoA) is converted to mevalonate by HMG-CoA reductase, the rate-limiting enzyme at the apex of this pathway, and the target of statin drugs. Mevalonate is then converted to isopentyl pyrophosphate, the 5-carbon basic isoprene unit. A series of enzymatic reactions convert isopentyl-PP to farnesyl pyrophosphate (a 15 carbon isoprenoid). Farnesyl-PP can then be converted to geranylgeranyl pyrophosphate (a 20 carbon isoprenoid) with the addition of another isopentyl-PP. In addition, farnesyl-PP can convert to dolichyl phosphate or cholesterol. In normal cells, isoprenoid products and cholesterol suppress HMG-CoA reductase through means of post-translational downregulation, creating a negative feedback loop. CAAX, C denotes cysteine, A denotes any aliphatic amino acid, and X may be any amino acid; FTase, farnesyltransferase; GGTase, geranylgeranyltransferase. Adapted from (10).

1.1.1 Mevalonate and Post-Translational Modifications

The mevalonate pathway regulates isoprenoid intermediates such as the 15-carbon farnesyl pyrophosphate (FPP), the 20-carbon geranylgeranyl pyrophosphate (GGPP), and dolichol pyrophosphate. Both FPP and GGPP serve as prenyl groups that can be added to cellular proteins[10]. Protein prenylation is the post-translational modification process of creating a lipidated hydrophobic domain by attaching an isoprene to the C-terminal of a protein. Usually, prenylation occurs on proteins containing a C-terminal CAAX motif (C denotes cysteine, A represents any aliphatic amino acid and X may be any amino acid)[11]. Functionally, the prenylation process permits the covalent attachment, localization, and intracellular trafficking of membrane-associated proteins by means of a lipid anchor[9]. Types of proteins that undergo prenylation modifications include small GTP-binding proteins, heme A, the γ subunit of G proteins, and nuclear lamins. Many proteins undergo geranylgeranylation, especially many of the small GTP-binding proteins like Rho, Rac, Rab[11]. These small GTP-binding proteins function in many diverse cellular processes ranging from regulating gene expression to protein trafficking, and inhibition of their activity can significantly alter cellular function of physiology[12]. For example, the reduced prenylation and consequent inhibition of Rho proteins leading to reduced proliferation, is thought to be an important anti-cancer effect of statins[13]. Another post-translational modification mediated by intermediates of the mevalonate pathway is *N*-linked protein glycosylation. Dolichol pyrophosphate acts as a carrier of oligosaccharides in the assembly of glycoproteins in the endoplasmic reticulum, and its availability represents a key factor

in the assembly of lipid-linked oligosaccharides[14]. Interestingly, it has been shown that some growth factor receptors, like the insulin-like growth factor-1 (IGF1) receptor, require *N*-glycosylation for its proper translocation to the cell surface[15].

1.2 STATINS AND IMMUNITY

Evidence from several large clinical trials have suggested that changes in lipid levels alone may not explain all of the beneficial effects of statins in reducing the risk of cardiovascular disease[3]. For example, results of the CARE[16] and HPS[17] trials showed that the cardiovascular benefit of statins did not correlate fully with the magnitude of cholesterol lowering. Moreover, organ transplant studies have shown that statins reduce the risk of transplant arteriopathy and stroke, which are not normally associated with elevated lipid levels[18,19]. These observations provide strong evidence in support of diffuse statin effects beyond simple lipid lowering.

1.2.1 Mevalonate and Immunity

Evidence from both basic and clinical research demonstrates that statins have many cholesterol-independent, or pleiotropic effects. These effects include improving endothelial vascular tone and decreasing surface expression of adhesion molecules, stabilizing atherosclerotic plaques, antithrombotic properties, decreasing oxidative stress, and anti-proliferative effects[20]. Recent studies indicate that statins also have anti-inflammatory and immunomodulatory properties. Simvastatin and atorvastatin have been shown to prevent cytokine-induced maturation of professional antigen-presenting

cells, and can subsequently inhibit T-cell proliferation[21]. These immunological effects of statins were reversed with cellular restoration of mevalonate or GGPP, providing support for the importance of protein prenylation in cholesterol-independent statin effects on immunity. Furthermore, inhibition of protein prenylation can reduce leukocyte adhesion, as well as reduce NADPH oxidase assembly to prevent the generation of reactive oxygen species (ROS) in endothelial cells[3]. Statins reduce levels of tumor necrosis factor (TNF) and interleukin (IL)-6 in lipopolysaccharide (LPS)-treated peripheral blood, which is also associated with statin-mediated decreases in protein prenylation[22]. In contrast to the anti-inflammatory properties of statins, a number of recent studies have shown that statins are able to enhance the production of the pro-inflammatory cytokines of the IL-1 family[23]. Fluvastatin has been shown to increase the secretion of the pro-inflammatory cytokines 1L-1β and IL-18 in *Mycobacterium tuberculosis* stimulated peripheral blood mononuclear cells[24]. In addition to fluvastatin, lovastatin can increase ROS and synergize with LPS to trigger IL-1β release[25]. These pro-inflammatory effects also appear to be dependent on prenylation because mevalonate treatment can attenuate statin-induced secretion of these pro-inflammatory cytokines[23,26]. Furthermore, inhibition of the prenylation enzyme geranylgeranyltransferase, mimics the effect of simvastatin on IL-1β and IL-18 secretion in THP1 monocytes[23].

Intriguingly, statin-mediated increases in IL-1β and IL-18 secretion is only seen in LPS or bacteria-treated (i.e. primed) immune cells. This is important as both IL-1β and IL-18 are synthesized in inactive precursor forms (i.e during priming) that require an

additional step of enzymatic processing for secretion of a biologically active protein[27]. Both of these pro-inflammatory cytokines can be activated through cleavage by caspase-1, which itself can be indirectly potentiated by priming signals like LPS and other bacterial ligands through cytosolic complexes called inflammasomes[28].

1.2.2 Caspase-1

Caspases are a family of cysteine proteases that are primarily known for their essential role in apoptosis[28]. However, not all caspases are involved in apoptosis. Caspase-1 is classified as an inflammatory caspase because of its regulation of pro-inflammatory cytokine activation. This response can also initiate a form of programmed cell death known as pyroptosis. Unlike apoptosis, pyroptosis mediated by caspase-1 is characterized by osmotic swelling and the subsequent rupture of the cell membrane, with the mitochondrial membrane remaining intact[29,30]. In contrast, apoptosis is considered to be immunologically silent and is dependent on caspase-3 processing[28]. Importantly, activation of caspase-1 does not always initiate pyroptosis, as this response is primarily used by immune cells to clear intracellular pathogens when infected by bacteria and viruses[30]. Often, activation of caspase-1 will promote inflammatory responses through cleavage of IL-1β.

Caspases share similarities in amino acid sequence, structure, and substrate specificity. They are all expressed as proenzymes that contain three domains: an NH_2-terminal domain, a large 20kD subunit, and a small 10kD subunit[31]. Since all of the domains are derived from the proenzyme and are cleaved at caspase consensus sites for

activation, caspases can be activated either autocatalytically, or in a cascade by enzymes with similar specificity. As proteases, caspases are among the most specific with an absolute requirement for cleavage after aspartic acid which sits in the P1 position. Recognition of at least four amino acids (P4 to P1) adjacent to the cleavage site is also required for efficient substrate processing. Different tetrapeptide motifs are recognized by different caspases, and specificity for each caspase is conferred primarily by the amino acid in the P4 site[32]. Recently it has been shown that sequences flanking the tetrapeptide also help to confer substrate specificity[33]. For caspase-1, the target sequence has been shown to be tryptophan/tyrosine at P4, valine at P3, any residue at P3, and aspartic acid at P1 (W/Y-V-X-D)[32]. These differences in motif recognition help to explain the diverse biological functions of caspases. While caspase-1 is well known to function in the maturation process of pro-inflammatory cytokines, it has also been shown to regulate protein translation[34], ubiquitination-proteasome degradation[35], DNA repair[36], stabilization of the cytoskeleton[37], and glycolysis[38]. As mentioned earlier, the activation of caspase-1 is mediated by cytosolic protein complexes known as inflammasomes[33].

1.3 THE INFLAMMASOMES

Activation of the inflammasome is a key function mediated by the innate immune system[39]. Several families of pathogen recognition receptors are important components of the inflammasome complex, including the nucleotide-binding domain, leucine-rich repeat containing proteins (NLRs) and the absent in melanoma 2 (AIM)-like receptors (ALRs)[40]. Inflammasomes are multimeric protein complexes that assemble in the cytosol

after sensing pathogen- or danger-associated molecular patterns (PAMPs and DAMPs, respectively). Different inflammasomes are activated by diverse ligands and triggers, and serve as a scaffold to recruit the inactive proenzyme caspase-1 (pro-caspase-1)[41]. One of the best characterized inflammasomes is the NLRP3 (nucleotide-binding domain, leucine-rich repeat containing protein, pyrin domain-containing-3) inflammasome[39]. While all inflammasomes recognize certain PAMPs and DAMPs, NLRP3 is distinct in its ability to recognize and respond to diverse stimuli, making it the most versatile inflammasome[42]. The mechanisms of NLRP3 inflammasome activation still lack consensus, but the majority of studies support a model where potassium efflux is a unifying factor[43]. Other stimuli include the generation of mitochondrial ROS, the release of mitochondrial DNA, and the release of cathepsins (lysosomal proteases that degrade internalized proteins) into the cytosol[44]. In most cell types, NLRP3 must be primed before activation of this inflammasome can occur (Figure 2)[45]. A prototypical example of such a priming event is the binding of LPS to toll-like receptor-4 (TLR4). This priming event increases the cellular expression of NLRP3 through nuclear factor-κB (NF-κB) signaling. Furthermore, recently it has been shown that priming can also rapidly induce the deubiquitination of NLRP3, independent of new protein synthesis to promote NLRP3 inflammasome activation[46,47]. Once primed, NLRP3 is ready to respond to stimuli to assemble the inflammasome complex. This assembly requires NLRP3 to associate with the adaptor protein ASC (apoptosis-associated speck-like protein containing a carboxy-terminal CARD), which is comprised of the caspase recruitment domain (CARD) linked to a pyrin domain[44]. The

NLRP3:ASC complex oligomerizes and associates with pro-caspase-1, thus forming active inflammasome complexes (NLRP3:ASC:caspase-1). The close proximity of pro-caspase-1 proteins then induces the autocatalytic cleavage of pro-caspase-1 into mature caspase-1. Currently, stimuli recognized as NLRP3 agonists include ATP, pore-forming toxins, crystalline substances, nucleic acids, and fungal, bacteria, and viral pathogens[39].

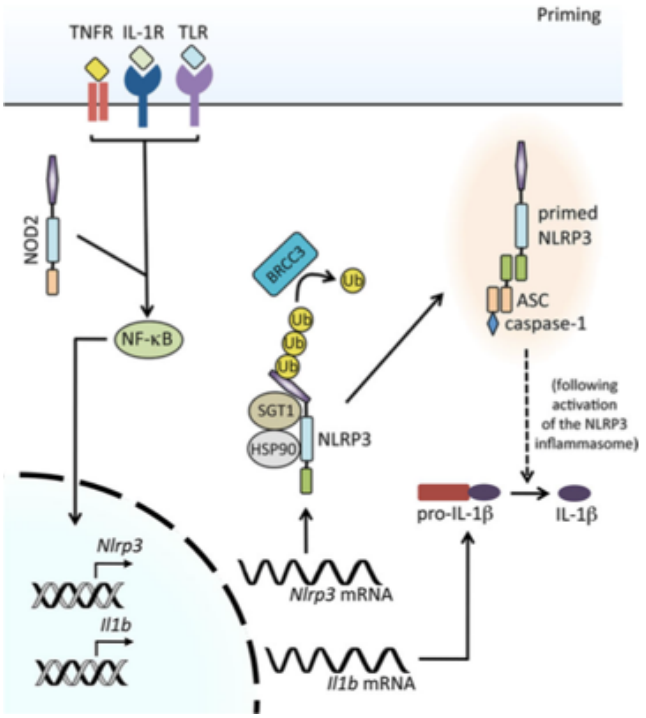

Figure 2| Steps to NLRP3 priming and inflammasome activation.

When pattern recognition receptors or cytokine receptors are activated by their respective ligands, causing the activation of the NF-κB transcription factor, this leads to the transcription and translation of NLRP3 and pro-IL-1β. NLRP3 activation requires that HSP90 and SGT1 dissociate from NLRP3, and that NLRP3 undergoes deubiquitinylation by the enzyme BRCC3. Once the inflammasome is fully assembled and activated forming a complex with ASC and caspase-1, active caspase-1 is now able to process pro-IL-1β into its mature form. Adapted from (45).

1.4 ADVERSE EFFECTS OF STATINS

Although statins are generally considered to be well-tolerated, their widespread use has revealed adverse effects that can result in intolerance, where the only recourse is discontinuation of statin treatment[48,49]. Of the reported side effects that include elevations in liver enzymes and increased risk for diabetes[50], the most common and potentially most serious side effect is myopathy or myotoxicity[5]. In randomized controlled trials, the incidence of statin myopathy ranges from 1.5-5%, while large community based studies have reported that 10-20% of patients experience mild muscle symptoms[51–53]. There are over 100 million statin prescriptions each year in the US alone and with new guidelines set forth by the American Heart Association, this has pushed the number of statin users to over 60 million in the US, with many other countries looking to follow this trend[54]. Therefore, statin-induced myopathy has the potential to affect millions of additional people[55].

1.4.1 Myopathy

The term myopathy defines a wide range of muscle-related symptoms. However, the terminology around statin-related adverse muscle events is variable and has changed over the years, likely contributing to the discrepancy in epidemiological data on the prevalence of statin myopathy. Recently, a European consensus panel has classified statin myopathy into six grades based on clinical symptoms and creatine kinase (CK) changes (Table 1)[56]. Generally, statin-induced myopathy ranges from clinically asymptomatic muscle disease with elevated serum CK, to muscle pain without changes in CK levels

(myalgia), to acute muscle pain accompanied with CK elevation (myositis), and to potentially life-threatening rhabdomyolysis[57]. Though many statin users will only experience mild symptoms, the development of myopathy can impact daily living and quality of life by affecting the patient's ability to accomplish simple tasks, or may prevent their participation in enjoyable recreational activities[58].

Table 1| A consensus group standardized classification of statin-related side-effects and their frequency. Adapted from (56).

Statin Myopathy Grade	Phenotype	Incidence	Definition
0	CK rise	1-26%	Asymptomatic
1	Mild Myalgia	0.3-33%	Muscle ache but no CK rise
2	Severe Myalgia	0.2-2/1000	Muscle ache; CK 4x the upper limit, resolves
3	Mild Myopathy	5/100000 patient years	Muscle ache; CK 4-10x the upper limit, resolves
4	Severe Myopathy	0.11%	Muscle ache; CK 10-50x the upper limit, resolves
5	Rhabdomyolysis	0.1-8.4/100000 patient years	CK 50x the upper limit or CK>10x with acute kidney injury
6	Autoimmune necrotizing myositis	2/1000000 per year	HMGR antibody in plasma, muscle biopsy; non-resolving

1.5 POSSIBLE MECHANISMS OF STATIN MYOPATHY

The etiology of statin-induced myopathy is still unclear, although it is likely that multiple pathophysiological mechanisms contribute to statin-induced myopathy. Many of the proposed mechanisms of statin myopathy are based on inhibition of HMGR in the mevalonate pathway. Potential factors contributing to statin myopathy include: alterations in muscle membrane function from reduced cholesterol production; reduced coenzyme Q10 (CoQ10) production resulting in impaired energy production and mitochondrial dysfunction; and alterations in gene expression of cellular components regulating apoptosis and protein degradation.

1.5.1 Alterations to the Muscle Membrane

Cholesterol and phospholipids are the two major lipid components of the cell membrane. As membrane cholesterol content dictates membrane stiffness and helps to maintain structural integrity, statin-dependent depletion of cholesterol in the cell membranes of myocytes can predispose to myopathy[59,60]. Such alterations can modulate the function of sodium, potassium and chloride channels, which will impact muscle membrane excitability and could help to explain the symptoms of muscle weakness and pain[61].

1.5.2 Mitochondrial Dysfunction

Early experimental data showed that some statin-treated patients had lower levels of circulating coenzyme Q10 and higher lactate/pyruvate ratios, which is an indicator of

abnormal mitochondrial function[62]. CoQ10, or ubiquinone, is a steroid isoprenoid synthesized through the mevalonate pathway that functions in the electron transport chain and participates in oxidative phosphorylation in the mitochondria[63]. Therefore, statin-mediated inhibition of CoQ10 production in muscle may be associated with reduced maximal mitochondrial oxidative phosphorylation capacity. In addition, reduced CoQ10 content has also been shown to promote the generation of ROS, as it also works as a potent antioxidant[64]. Some clinical studies have shown that CoQ10 co-administration with high-dose statins improve the perception of statin-related muscle pain; however, many other studies do not support any benefit from CoQ10 supplementation when compared to placebo in patients on commonly prescribed statin doses[65]. In addition to lowering CoQ10, it has been proposed that statins also induce mitochondrial depolarization. Acute application of simvastatin has been shown to cause a rapid dose-dependent depolarization of mitochondrial membranes in bundles of muscle fibers[66]. This depolarization would suggest that statins can mediate the uncoupling of mitochondrial oxidative phosphorylation[67]. These alterations in mitochondrial function can lead to an increase in cytoplasmic calcium ions and sarcoplasmic reticulum calcium overload[66]. When overloaded, the sarcoplasmic reticulum may spontaneously release calcium to generate a calcium wave, which may account for the cramps and myalgia described by statin myopathy patients. It has also been shown *in vitro* and *in vivo* with rats that fluvastatin and atorvastatin treatment increases resting cytosolic calcium, suggesting defects in calcium homeostasis[68]. Such changes in calcium homeostasis could lead to

caspase-3 activation and induce apoptosis through Bcl-2, a regulatory protein of cell death[69]. There is additional evidence that shows statin treatment can also increase lipid peroxidation and oxidative stress. Kwak et al. showed that exposing human muscle cells to simvastatin resulted in impaired ADP-stimulated mitochondrial respiration, increased ROS production, and activation of apoptosis[70].

1.5.3 Dysregulation of Apoptosis and Protein Degradation

Statins have been shown to induce apoptosis in a variety of cell types[58]. As the mitochondria plays an important role in regulating apoptosis, any disruption to mitochondrial function can propagate the apoptotic signaling pathway. Interestingly, the addition of mevalonate prevents statin-induced apoptosis and activation of caspase-3, which strongly suggests that the depletion of downstream products of the mevalonate pathway induces muscle cell apoptosis, at least *in vitro*[71,72].

In cell culture, statins have been shown to diminish muscle oxygen consumption, promote mitochondrial permeability, decrease ATP levels, and generate apoptotic proteins[73]. In animal models, some studies have shown statin treatment can increase ROS production and mitochondrial swelling. However, many other animal studies reveal no changes in mitochondrial enzyme activity during statin treatment. Results from human studies have been even more inconsistent, with only some showing that statin patients have decreased CoQ10, elevated lipids, decreased enzyme activities, and impaired maximal oxygen uptake in muscle. The inconsistency in the data surrounding the pathogenesis of statin-induced myopathy clearly indicates that more work needs to be

done to piece together the possible mechanisms at work (Figure 3). Some of this discrepancy may be attributable to differences in models of statin myotoxicity. There may be intrinsic differences in the progression of myopathy when looking at overt muscle cell death, which is more relevant to rhabdomyolysis, compared to low-level myopathy, which is more common. Intriguingly, the effects of statins on altering mitochondrial function, increasing ROS, and reducing intracellular ATP levels are all features indicative of the stimuli and processes that activate the NLRP3 inflammasome, possibly implicating a new immune link between statin treatment and myopathy.

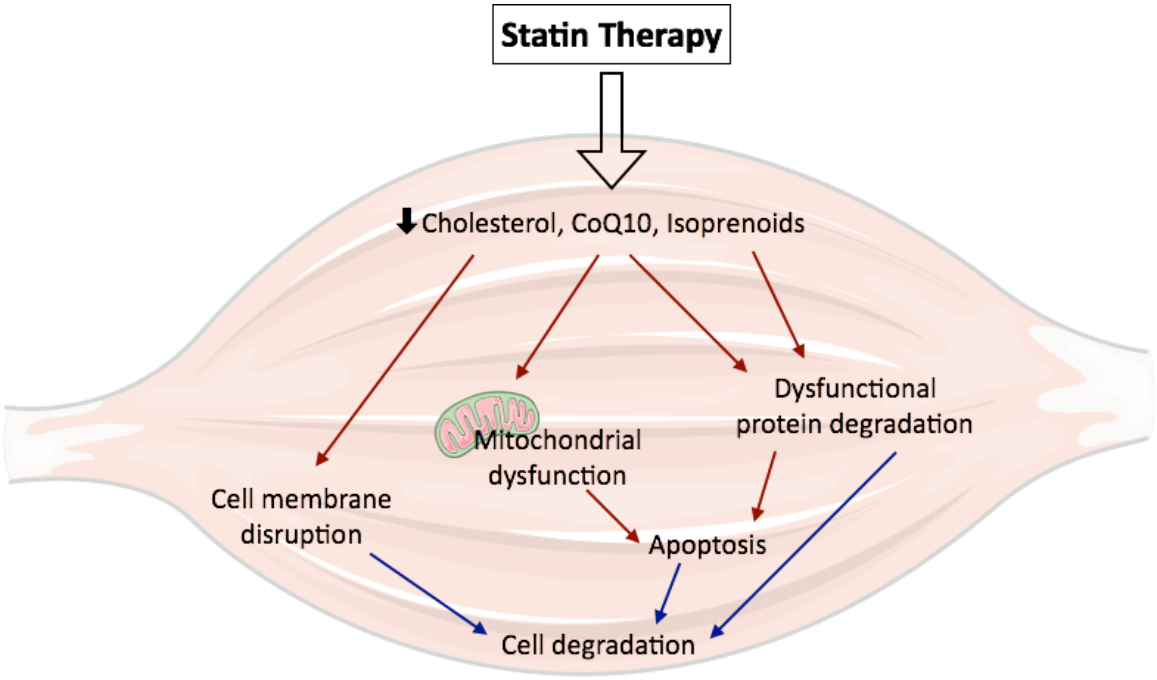

Figure 3| Current theories of the possible mechanisms contributing to statin myopathy.

1.6 MUSCLE GROWTH AND DAMAGE

Skeletal muscle maintenance involves interconnected signals that coordinate hypertrophic and atrophic messages, culminating in a balance between muscle protein synthesis and breakdown.

1.6.1 IGF1/Akt Signaling Cascade

Skeletal muscle hypertrophy, characterized as an increase in the size of pre-existing myofibers, involves increased protein synthesis, and can be induced by many anabolic stimuli[74]. Signaling via IGF1 augments muscle growth and inhibits breakdown. *In vitro* and *in vivo*, IGF1 stimulates both proliferation and differentiation of muscle cells[75–77]. Binding of IGF1 to its receptor leads to activation of its intrinsic tyrosine kinase and autophosphorylation, thus generating docking sites for insulin receptor substrate (IRS) (Figure 4)[78]. Phosphorylated IRS then works to recruit and activate phosphatidylinositol-3-kinase (PI3K), which phosphorylates membrane phospholipids to generate phosphoinositide-3,4,5-triphosphate (PIP3). PIP3 acts as a docking site for the kinases phosphoinositide-dependent kinase 1 (PDK1) and Akt. Activation of Akt by phosphorylation at threonine 308, leads to inhibition of protein degradation through phosphorylation and nuclear exclusion of Forkhead box gene group O (FOXO) transcription factors, and stimulation of protein synthesis via the mammalian target of rapamycin (mTOR) and glycogen synthase kinase 3β (GSK3β). mTOR can form two different protein complexes: the rapamycin-sensitive mTORC1 and the rampamycin-insensitive mTORC2. mTORC1 is important for phosphorylating S6 kinase (S6K) which goes

on to stimulate factors involved in translation initiation and elongation to promote protein synthesis. mTORC1 also phosphorylates the inhibitory binding proteins of eukaryotic translation initiation factor 4E (eIF4E), allowing this translation initiation machinery to work. Activity of the IGF1/Akt pathway is controlled by several feedback loops. Negative feedback involves S6K, which inhibits IRS through serine phosphorylation at multiple sites that lead to degradation and altered cell localization. Positive feedback involves mTORC2, which phosphorylates Akt at serine 473 and is needed for maximum activation of Akt and suppression of FOXO activity.

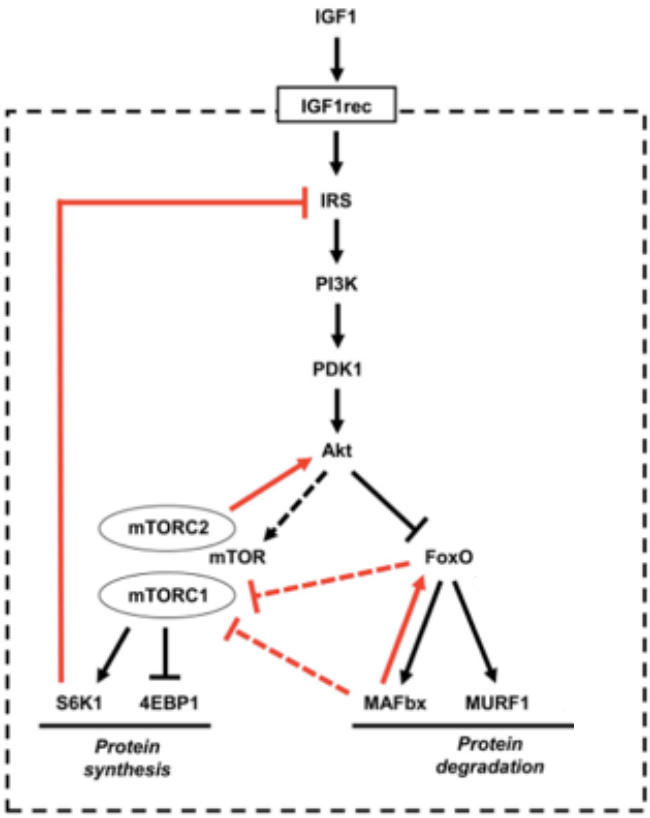

Figure 4| Simplified insulin-like growth factor 1 (IGF1) signaling pathway.

IGF1 binds to the insulin-like growth factor receptor (IGF1rec), where IRS1 is phosphorylated leading to subsequent phosphorylation and activation of phosphatidylinositol 3-kinase (PI3K), resulting in phosphorylation of Akt at serine 308 by PDK1. All these steps take place at the inner surface of the plasma membrane. Akt is able to inhibit protein degradation by phosphorylating the transcription factors of the FOXO family. It is also able to stimulate protein synthesis indirectly via mTOR. mTORC1 phosphorylates S6 kinase (S6K) which stimulates factors involved in translation initiation and elongation. Furthermore, mTORC1 activates the eukaryotic translation initiation factor 4E (eIF4E) by phosphorylating its inhibitory eIF4E-binding proteins (4EBPs). mTORC2 also positively feeds back to Akt by phosphorylating Akt at serine 473, allowing for maximum activation of Akt. Overall, products of the FOXO arm are able to modulate the effects achieved through the mTOR branch of the pathway. Adapted from (78).

The IGF1/Akt pathway shares most of its components with the insulin/Akt pathway, and the two pathways intersect at various points. Recently, Mullen and colleagues have shown that the disruption of IGF1/Akt signaling is a causative factor in simvastatin-induced mitochondrial dysfunction in C2C12 myotubes, and that HepG2 liver cells are protected from toxicity by maintaining IGF1/Akt signaling after simvastatin treatment[79]. However, the mechanisms behind how statins can impair the IGF1/Akt pathway remain unknown. There is some evidence to suggest a depletion of functional IGF1 receptors at the cell surface of melanoma cells contributes to IGF1/Akt signaling defects[15]. Carlberg et al. demonstrated that statin-mediated depletion of IGF1 receptor *N*-glycosylation significantly contributed to reduced levels of functioning IGF1 receptors as mevalonate was able to restore the expression of receptors at the cell surface, and the number of IGF1 binding sites.

1.6.2 Muscle Ubiquitin Ligases

Skeletal muscle atrophy is characterized by a shift towards protein degradation. It has been shown that the proteolysis observed in atrophy occurs in part due to the activation of ubiquitin-mediated proteasomal degradation[80]. This ubiquitin-proteasome system is characterized by the concerted action of ubiquitin-conjugating enzymes that link chains of the polypeptide co-factor ubiquitin on to proteins to mark them for degradation[81]. The tagging process allows them to be recognized by the proteasome, a very large multi-catalytic protease complex that degrades proteins into small peptides[82]. Although there are three enzymatic components required for linking chains of ubiquitin on to proteins destined for degradation, the E3 ubiquitin ligase is the key component of the conjugation apparatus that confers specificity to the system[83]. E3 ubiquitin ligases works to couple ubiquitin and the actions of E1 (ubiquitin-activating enzyme) and E2 (ubiquitin-carrier proteins) to the protein substrate. Both muscle RING finger-containing protein 1 (MuRF-1) and muscle atrophy Fbox protein (MAFbx) are genes that encode for muscle-specific E3 ubiquitin ligases. MuRF-1 localizes to the sarcomere and has been shown to bind to myosin heavy chain and myosin light chain, suggesting that MuRF-1 induces muscle atrophy by directly attacking the thick filament of the sarcomere and causing the proteolysis of myosin proteins[74,84,85]. On the other hand, MAFbx (also called atrogin-1) has been shown to be a E3 ligase for eIF3f, a protein initiation factor[74]. This finding would suggest that atrogin-1 activity results in atrophy through the downregulation of protein synthesis.

1.6.3 Ubiquitin Ligases in Statin Myopathy

Multiple models of atrophy including denervation, high-dose dexamethasone treatment, treatment with inflammatory cytokines, and immobilization all induce the transcriptional upregulation of MuRF1 and atrogin-1 (collectively referred to as atrogenes). However, other models of atrophy like Duchenne muscular dystrophy, a genetic disease resulting in muscle degeneration, show no dependence on altered atrogin-1 expression[86]. This suggests that atrogin-1 is not just a general marker of muscle atrophy and damage. Interestingly, statins have also been shown to induce the expression of atrogin-1 and MuRF-1 both *in vitro* and *in vivo*. Mallinson et al. showed that rats treated with simvastatin have increased atrogin-1 and MuRF-1 gene expression[87]. Similarly, another study by Hanai et al. showed that patients presenting with statin myopathy have increased atrogin-1 mRNA expression, and that lovastatin-treated C2C12 myotubes show significantly higher levels of atrogin-1 mRNA and protein[88]. Importantly, this study also showed that myotubes from atrogin-1 null mice were resistant to lovastatin-induced myotube atrophy. In addition, increased atrogin-1 expression in statin-treated cultured mouse myotubes has been shown to result from a geranylgeranylation defect, where the expression of atrogin-1 can be prevented when geranylgeranol is present[79,89]. These data show that statin-induced lowering of isoprenoids required for protein prenylation increase atrogenes and support using atrogin-1 and MuRF-1 as markers of statin-induced myopathy.

1.6.4 Regulation of Atrogin-1 and MuRF-1

The transcription of atrogin-1 and MuRF-1 is most commonly regulated by FOXO transcription factors. Normally, the upregulation of these ubiquitin ligases are blocked by Akt through negative regulation of the FOXO family transcription factors[90–92]. Activation of the PI3K/Akt pathway allows Akt to phosphorylate FOXO transcription factors to promote their export from the nucleus into the cytoplasm, thereby preventing the transcription of atrogin-1 and MuRF-1[93]. There are three members of the FOXO family found in skeletal muscle: FOXO1, FOXO3a, and FOXO4. In C2C12 myotubes, the expression of either constitutively active FOXO1 or FOXO3a increased the amount of E3 mRNA and decreased myofiber size[90]. In addition, FOXO1 transgenic mice showed significantly reduced muscle mass and fiber atrophy[94]. Similarly, knocking down FOXO expression is able to block the upregulation of atrogin-1 expression during atrophy[95].

Additionally, atrogin-1 and MuRF-1 can also be regulated by the NF-κB transcription factor. *In vivo*, activation of NF-κB has been shown to regulate skeletal muscle atrophy through regulation of MuRF-1 expression[96]. Moreover, activation of the p38 stress kinase pathway and subsequent NF-κB activation, has also been shown to increase atrogin-1 and MuRF-1 gene expression, and reduce myofibrillar protein in differentiated C2C12 myotubes[97].

2.0 RATIONALE, HYPOTHESES AND RESEARCH AIMS

2.1 RATIONALE

Statins have been reported to activate the NLRP3 inflammasome through reduced protein prenylation in immune cells. In addition, protein prenylation has also been linked to increased atrogin-1 expression in models of statin myopathy[88]. Moreover, previous work in the Schertzer lab has shown that statin-mediated NLRP3 activation promotes insulin resistance in adipose tissue[98]. As there are many similarities between IGF1 and insulin signaling pathways, it is possible that statins may have a similar NLRP3-dependent effect on IGF1 signaling, leading to increased expression of the atrophy-related genes atrogin-1 and MuRF-1. These support the notion of potential links between statins, the NLRP3 inflammasome, and myopathy. Therefore, the present studies were undertaken to ascertain if the NLRP3 inflammasome contributes to aspects of statin-induced myopathy, and to establish if protein prenylation regulates NLRP3/caspase-1 activity in muscle cells, where statins promote markers of myopathy via inhibition of the IGF1/Akt/FOXO signaling pathway.

2.2 HYPOTHESIS

We hypothesize that activation of the NLRP3/caspase-1 inflammasome in muscle cells will promote statin-induced myopathy, and that inhibition of the inflammasome will aid in myopathy prevention. Furthermore, we hypothesize that the effects of statins on NLRP3 and atrogene expression are dependent on isoprenoids used for protein prenylation.

2.3 RESEARCH AIMS

Using C2C12 muscle cells, our research objectives were:

1) To establish a testable *in vitro* model of statin-induced myopathy.

2) To determine if statins promote NLRP3 inflammasome activity during statin treatment.

3) To investigate the role of the NLRP3 inflammasome in promoting markers of statin-induced myopathy.

4) To determine if any observed effects are dependent on cholesterol or isoprenoids.

3.0 MATERIALS AND METHODOLOGY

3.1 REAGENTS AND ANTIBODIES

Chloroform and anhydrous ethyl alcohol were from Anachemia, and methanol and isopropyl alcohol were from BDH VWR Analytical. TRIzol® was purchased from Ambion (Thermo Fisher Scientific). Ultrapure water, DNAse I 10x reaction Buffer, DNAse I amplification grade, 5x first strand buffer, dNTPs (dATP, dTTP, dGTP, dCTP), and SuperScript III were from Invitrogen (Thermo Fisher Scientific). 10x PCR gold buffer, $MgCl_2$, and AmpliTaq Gold were from Applied Biosystems. Oligonucleotide primers for cDNA synthesis (random hexamers, random pentadecamers, and Oligo-dT(18)) were obtained from the McMaster University MOBIX Lab. All RT-PCR (real-time polymerase chain reaction) primers were purchased from TaqMan (Thermo Fisher Scientific). TEMED was purchased from Bio-Rad. DMSO, NaF, Na_3VO_4, Triton-100, dithiothreitol (DTT), Tween-20, NP-40, ammonium persulfate ($(NH_4)_2S_2O_8$), LONG® R^3 IGF1, and 25-hydroxycholesterol were purchased from Sigma-Aldrich. c*O*mplete™ protease inhibitor cocktail tablets were purchased from Roche. Fluvastatin (sodium salt), atorvastatin (calcium salt), pravastatin (sodium salt), and geranylgeranyl pyrophosphate (ammonium salt) (GGPP) were purchased from Cayman Chemical. Cerivastatin sodium was purchased from LKT Laboratories. LPS (*E.coli* 0111:B4) and Z-VAD-FMK were purchased from InvivoGen. Z-WEHD-FMK was purchased from Abcam, and Z56765797 was from Enamine. Bicinchoninic acid (BCA) assays, albumin standards, and ECL western blotting substrate were purchased from Pierce Thermo Fisher Scientific. Primary antibodies for polyclonal anti-phospho-Akt

(Ser473), anti-phospho-Akt (Thr308), Akt anti-GAPDH, and anti-phospho-FOXO1 (Thr24)/FOXO3a (Thr32) were obtained from Cell Signaling Technology.

3.2 CELL CULTURE

3.2.1 Cell Culture Reagents

Dulbecco's modified eagle medium (DMEM), fetal bovine serum (FBS), horse serum, phosphate-buffered saline (PBS), trypsin and antibiotic solution were from Gibco© ThermoFisher Scientific. Cell growth media was composed of DMEM supplemented with 10% (v/v) FBS and 1% (v/v) antibiotic (10,000units/ml of penicillin, 10,000 ug/mL of streptomycin, and 25 ug/mL of amphotericin B) solution. Myoblast differentiation media was composed of DMEM supplemented with 2% (v/v) horse serum and 1% (v/v) antibiotic solution.

3.2.2 Cell Culture Procedures

All experiments were conducted in the mouse C2C12 cells, a C3H muscle myoblast cell line (Sigma Cat No: 91031101). Myoblast cells were grown in cell growth media and maintained in a humidified atmosphere of 5% CO_2 at 37°C. After myoblast cells reached 90-100% confluence, differentiation into myotubes was initiated by switching the growth media to differentiation media. Using an OMAX A3590U microscope, cells were monitored daily for fusion of myoblasts into myotubes (fiber-like structures). On day 3 or 4 of differentiation, cells were treated under various conditions in differentiation media. Figure 5 illustrates the general treatment protocols used.

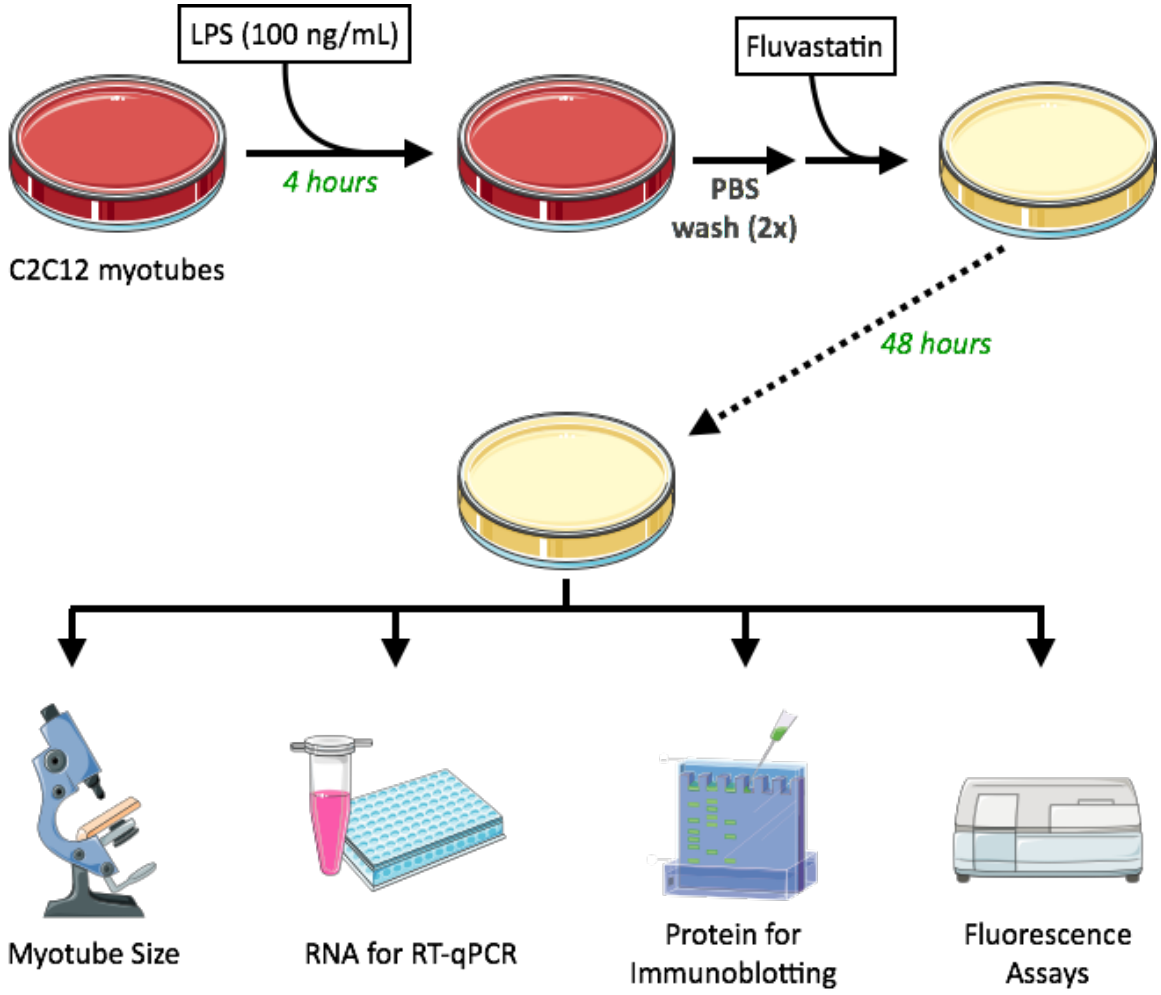

Figure 5| *Illustration of treatment protocol.*

If pretreatment was required, C2C12 myotubes were treated for 4 hours with LPS. Cells were washed twice with PBS before fresh media was added. Fluvastatin treatment media alone, or containing IGF1, GGPP, caspase-1 or NLRP3 inhibitors, were placed on myotubes for 48 hours before RNA or protein was extracted for analysis.

3.3 GENE EXPRESSION ANALYSIS

3.3.1 RNA Extraction from Cells

C2C12 myotubes were scrapped and triturated with a 1 mL pipette tip in TRIzol® for extraction of RNA. To begin the extraction process, 200 µL of chloroform was added per 1 mL of TRIzol® reagent. The samples were then mixed vigorously and centrifuged at 4°C for 15 minutes at 12,000 x g. The upper aqueous phase was then transferred into a fresh tube. The RNA was precipitated from the aqueous phase by mixing with isopropyl alcohol (500 µL of alcohol per 1 mL TRIzol®). The samples were then incubated at room temperature for 10 minutes, and centrifuged at 4°C at 12,000 x g for 10 minutes. The supernatant was discarded and the gel-like, RNA pellet was washed twice with 75% anhydrous ethyl alcohol. The pellet was spun down after each wash at 7,500 x g at 4°C for 5 minutes. Following the last wash, any remaining ethanol was allowed to evaporate before dissolving the RNA pellet in UltraPure, distilled water.

3.3.2 cDNA Synthesis

RNA concentration was measured by spectrophotometry, using the NanoDrop 2000 (Thermo Fisher Scientific). To eliminate single- and double-stranded DNA from each sample, 1 µg of RNA was mixed with 0.5 µL of DNAse I 10x Reaction Buffer (200 mM Tris-HCl (pH 8.4), 20 mM $MgCl_2$, 500 mM KCl) and 0.5 µL of DNAse I Amplification Grade for 15 minutes at room temperature. 0.5 µL of EDTA (25 mM), 0.5 µL of random hexamer primers (250 ng/µL) and 0.5 µL of dNTPs (10 mM) were added to each sample. The samples were incubated in the SimpliAmp Thermal Cycler (Applied Biosystems) at 95°C for 10 minutes

to inactivate DNAse I, then at 55°C for 10 minutes to anneal the primers. cDNA was synthesized by adding 2 µL of 5x First Strand Buffer (250 mM Tris-HCl (pH 8.3), 375 mM KCl, 15 mM $MgCl_2$), 0.5 µL of DTT (0.1 M), 0.5 µL of UltraPure, distilled water, and 0.5 µL of SuperScript™ III to each sample, and incubating the samples in the thermal cycler for 50 minutes at 55°C, followed by 15 minutes at 70°C. All cDNA samples were diluted 1:25 in UltraPure distilled water and stored at -20°C.

3.3.3 RT-qPCR Reactions

10 µL of each cDNA sample was mixed with 10 µL of master mix (per sample: 5.1 µL UltraPure water, 2 µL 10x PCR Gold Buffer, 2 µL $MgCl_2$, 0.4 µL dNTPs (10 mM), 0.2 µL TaqMan® primer, and 0.1 µL AmpliTaq® Gold). For a full list of primers used, refer to Table 2. RT-PCR was performed using a Rotor-Gene Q (Qiagen) set to run for 50 cycles (95°C for 10 seconds, then 58°C for 45 seconds). All gene expression data were normalized to the respective RPLP0 (ribosomal protein, large, P0) housekeeping control for each sample and analyzed using the comparative CT method.

Table 2| Primers used in RT-qPCR.

Primer	Gene	Catalogue Number
Rplp0	Ribosomal protein (housekeeper)	Mm01974474
Fbxo32	atrogin-1, MAFbx	Mm00499523
Trim63	MuRF-1	Mm01185221
Il6	IL-6	Mm00446190
Il1β	IL-1β	Mm00434228
Il18	IL-18	Mm00434226
Tnfα	TNFα	Mm00443258
Nod1	NOD1	Mm00805062
Nod2	NOD2	Mm00467543
Tlr4	TLR4	Mm00445273
Mefv	pyrin	Mm01342372
Nlrp3	NLRP3	Mm00840904

Table 3| Antibodies utilized in immunoblotting.

Primary Antibody	Dilution	Catalogue Number
Phospho-Akt (Ser473)	1:1000	CST #4058
Phospho-Akt (Thr308)	1:1000	CST #4056
Akt	1:1000	CST #9272
Phospho-FOXO1(Thr24)/FOXO3a(Thr32)	1:1000	CST #9464
GAPDH	1:1000	CST #5174

3.4 PROTEIN ANALYSIS

3.4.1 Protein Extraction from Cells

C2C12 cells were lysed in SBJ lysis buffer (50 mM HEPES, 150 mM NaCl, 100 mM NaF, 10 mM NaP_2O_7, 5 mM EDTA·$2H_2O$, and 250 mM sucrose) supplemented with 1% Triton-100, 200 mM Na_3VO_4, and a quarter tablet (in 10 mL of buffer) of protease inhibitor cocktail. 300 µL of lysis buffer was used per 4 cm^2 of surface area. Adherent cells were scrapped using a cell scrapper and transferred to a fresh tube. Samples were passed through a 26-gauge needle to ensure all cells were appropriately lysed. The samples were then spun down at 13,000 x g for 15 minutes at 4°C to remove all non-solubilized debris from the final lysate preparations. All samples were stored at -80°C until needed.

3.4.2 Total Protein Measurements

Protein concentrations were measured by bicinchoninic acid (BCA) assay. Lysate samples were diluted 1:5 in Milli-Q® water to prepare 25 µL for the assay. Proteins standards were prepared using 2 mg/mL albumin diluted in Milli-Q® water. The assay was run using a clear 96-well plate. Following the protocol outlined by Pierce, the BCA reagent solution was made by mixing Reagent A and Reagent B in a 50:1 ratio. 200 µL of the BCA reagent solution was added to each sample; samples were run in duplicates. Absorbance readings were taken at 562 nm using the Synergy H4 Hybrid Reader (BioTek, Fischer Scientific) after the samples had incubated with the BCA reagent solution for 30 minutes at 37°C. Total protein concentration values were then interpolated using Prism 6.0 software, based on the standard curve generated.

3.4.3 Immunoblotting

Protein lysates were prepared for immunoblotting by adding 4x Laemmli buffer (8% SDS, 40% glycerol, 240 mM Tris-HCl (pH 6.8), 10% 2-mercaptoethanol, and 0.02% bromophenol blue) 1:4 to lysate samples. Lysate samples were then boiled at 95°C for 5 minutes to denature proteins. 10-20 μg of protein was loaded onto a 10% SDS-PAGE gel, and electrophoresis was carried out at 100V for approximately 1 hour and 45 minutes, or until the dye front reached the bottom of the gel. Protein was transferred onto a PVDF membrane using the Trans-Blot Turbo System (Bio-Rad) set at 25V for 25 minutes. Membranes were then blocked in 5% bovine serum albumin (BSA) for 1 hour before being incubated with primary antibody overnight at 4°C. All primary antibodies and their respective dilutions are listed in Table 3. Membranes were washed in Tris-buffered saline with 0.5% Tween-20 (TBS-T) four times, each for 10 minutes. After washing, membranes were incubated with the appropriate horseradish-peroxidase (HRP)-conjugated species-specific IgG secondary antibodies. Secondary antibodies were diluted 1:5000 in TBS-T and incubated with membranes for 1 hour at room temperature. Membranes were again washed in TBS-T four times for 10 minutes each before developing the membrane using Pierce ECL Western Blotting Substrate. ECL solution was prepared according to manufacturer directions and membranes were incubated in ECL solution for at least 2 minutes before detection in the Bio-Rad Imager. Band intensities were visualized using Bio-Rad Image Lab and quantified using NIH Imaging Software (ImageJ).

3.5 MYOTUBE DIAMETER ANALYSIS

Images of cultured myotubes were taken on an OMAX microscope using Toupview 3 at 40x magnification. Myotube diameter measurements were obtained using NIH Image software (ImageJ). Pixel to length scale was determined by calibrating a hemocytometer image taken at 40x magnification. To analyze myotube diameters, three short-axis measurements were taken along the length of a given myotube, and an average of these three values was used to determine a single myotube diameter value. A total of 100 myotubes were measured and replicated in three independent experiments.

3.6 CASPASE-1 ACTIVITY ASSAYS

3.6.1 FAM-FLICA Caspase-1 Assay

Presence of active caspase-1 was quantified using the FAM-FLICA Caspase-1 Assay Kit, a fluorescence-based assay. This assay kit uses the FLICA probe, which is a non-cytotoxic fluorescently-labelled probe that covalently binds only to active caspase enzymes. Active caspase enzymes exhibit catalytic and substrate specificities for short, tetra-peptide amino acid sequences. This allows for the generation of peptide sequences that can bind competitively to specific caspases. For caspase-1, the FAM-YVAD-FMK (carboxyfluorescein-YVAD-fluroromethyl ketone) reporter dye was used and the assay was run according to the manufacturer's instructions (ImmunoChemistry Cat No: #98). Briefly, C2C12 myoblasts differentiated and treated in a black, clear-bottom 96-well plate. To measure caspase-1, 1X FLICA solution was added to each well and allowed to incubate with the cells for 60 minutes at 37°C, ensuring the plate was protected from light. The

plate was mixed gently by tapping every 10 minutes to ensure even distribution of FLICA in the wells. After the one-hour incubation, the assay plate was centrifuged at 1500 rpm for 5 minutes to sediment any loose floating cells and the excess media was then aspirated off. Cells were then incubated at 37°C in 200 µL of fresh differentiation media for 20 minutes to allow for any unbound FLICA to diffuse out. This wash step, from centrifugation to incubation, was repeated twice. Following the three washes, 50 µL of PBS was added to each well. Fluorescence intensity was measured using the Synergy H4 Hybrid Reader set to excite at a wavelength of 488 nm and read an emitted wavelength of 530 nm. Following fluorescence quantification, the cells were then lysed in 50 µL of SBJ lysis buffer supplemented with 1% Triton-100, 200 mM Na_3VO_4, and a quarter tablet of protease inhibitor cocktail for total protein measurements by BCA. All fluorescence values were then normalized to their respective total protein values and presented as relative fluorescence units (RFU) per µg of protein.

3.6.2 Fluorometric Caspase-1 Activity Assay

Enzymatic activity of caspase-1 was measured using the BioVision Caspase-1/ICE Fluorometric Assay Kit. This assay detects the cleavage of substrate YVAD-AFC (AFC: 7-amino-4-trifluoromethyl coumarin). Intact YVAD-AFC emits blue light, but upon cleavage by caspase-1, free AFC emits a yellow-green fluorescence. The assay was prepared according to manufacturer's instructions with modifications (BioVision Cat No: K110-200). To prepare cell lysates for the assay, treated myotubes were lysed in Aussie buffer (50 mM KH2PO4, 4 mM EDTA, 1.15% KCl, and 0.5 mM DTT) supplemented with a quarter

tablet (in 10 mL of buffer) of protease inhibitor cocktail. Samples were passed through a 26-gauge needle to ensure all cells were appropriately lysed, and centrifuged at 4°C at 13,000 x g for 15 minutes to sediment the cell debris. The supernatant was then transferred to a fresh Eppendorf tube and stored at -80°C if the assay was not being performed on the same day. Before preparing the enzymatic assay, total protein of each sample was measured by BCA (described previously). Loading samples were then prepared to ensure that equal amounts of protein were loaded between samples. In a black, 96-well plate, 50 µL of cell lysate was added to 50 µL of 2X Reaction Buffer (containing 10 mM DTT). 50 µL of Aussie Buffer was added to 2X Reaction Buffer for a negative control. 5 µL of 1 mM YVAD-AFC substrate was then added to each sample. The plate was read in kinetic mode at an excitation of 400 nm and an emission of 505 nm for 4.5 hours at 37°C. Fluorescence measurements were taken every 30 minutes. To determine the fold increase in caspase-1 activity, treated samples were compared with untreated control samples.

3.7 STATISTICAL ANALYSES

Statistical analyses were carried out using Prism 6.0 software (GraphPad Software, San Diego, CA). Groups were compared using one-way analysis of variance (ANOVA) Tukey post hoc analysis, two-way ANOVA Tukey's multiple comparison test, or Student's T-Test. Unpaired Student's T-Test was used when comparing two means. For example, basal Akt phosphorylation was compared between untreated myotubes and fluvastatin (1 µM)

treated myotubes by T-Test. One-way ANOVA was used when comparing more than two means. For example, gene expression of a given cytokine (such as IL-6) was compared irrespective of other cytokines, where the three groups (untreated controls, 4-hour LPS treated, and 4-hour LPS pretreatment with removal for 48 hours) were analyzed by one-way ANOVA. Two-way ANOVA was used to test for significant interaction between multiple means. For example, we examined how the categorical factors of no pretreatment and LPS pretreatment on different doses of fluvastatin-induced atrogene expression. All results are expressed as mean ± SEM (standard error of the mean). Clinical data from patient samples are expressed as mean ± SD (standard deviation). Each individual treatment well was considered an independent experiment, and a minimum of two cell passages were used to generate the data in each figure, except for data shown in Figure 8C and 13B where experiments were performed under one cell passage. $p<0.05$ was considered to be statistically significant.

4.0 RESULTS

4.1 Priming of the NLRP3 inflammasome enhances the effect of fluvastatin in myotubes

We sought to investigate the possible contribution of the NLRP3 inflammasome in muscle cell autonomous responses that contribute to statin-induced myopathy. As such, we first addressed the concept of an adequate *in vitro* muscle cell model by taking into account the unique two-step priming/activation mechanism of the NLRP3 inflammasome. Using C2C12 myoblasts differentiated into myotubes, the inflammasome was primed by treating myotubes with 100 ng/mL of LPS. LPS exposure for 4 hours significantly increased transcript levels of the inflammasome components NLRP3, pyrin, and pathogen recognition receptor NOD1 (Figure 6A), as well as the pro-inflammatory cytokines IL-1β, IL-6 and TNFα (Figure 6B). As increased NLRP3 expression is a key component of priming this inflammasome in immune cells[99], these data show that LPS is also a sufficient stimulus to prime the NLRP3 inflammasome in muscle cells. Even without LPS exposure, 10 μM of fluvastatin treatment of C2C12 myotubes for 48 hours was able to significantly increase expression of the muscle E3 ubiquitin ligases, atrogin-1 and MuRF-1 (Figure 7A, 7B). Importantly, LPS pretreatment for 4 hours promoted a significant increase in the expression of both atrogin-1 and MuRF-1 at a lower fluvastatin dose (1 μM) (Figure 7A, 7B). This effect occurred despite the LPS being removed after 4 hours prior to the 48-hour fluvastatin exposure in C2C12 myotubes. These data are consistent with a model where myotubes become more sensitive to fluvastatin-induced atrogene induction when the NLRP3 inflammasome is primed. We used this model of a 4-hour LPS pretreatment

followed by a 48-hour fluvastatin treatment in C2C12 myotubes in all subsequent experiments. This model of LPS-primed muscle cell autonomous induction of atrogenes is not unique to fluvastatin. Atorvastatin and cerivastatin treatment also significantly increases atrogin-1 expression (Figure 8A, 8B), with cerivastatin being more potent than both fluvastatin and atorvastatin. Interestingly, pravastatin treatment did not alter atrogene expression in C2C12 myotubes (Figure 8C).

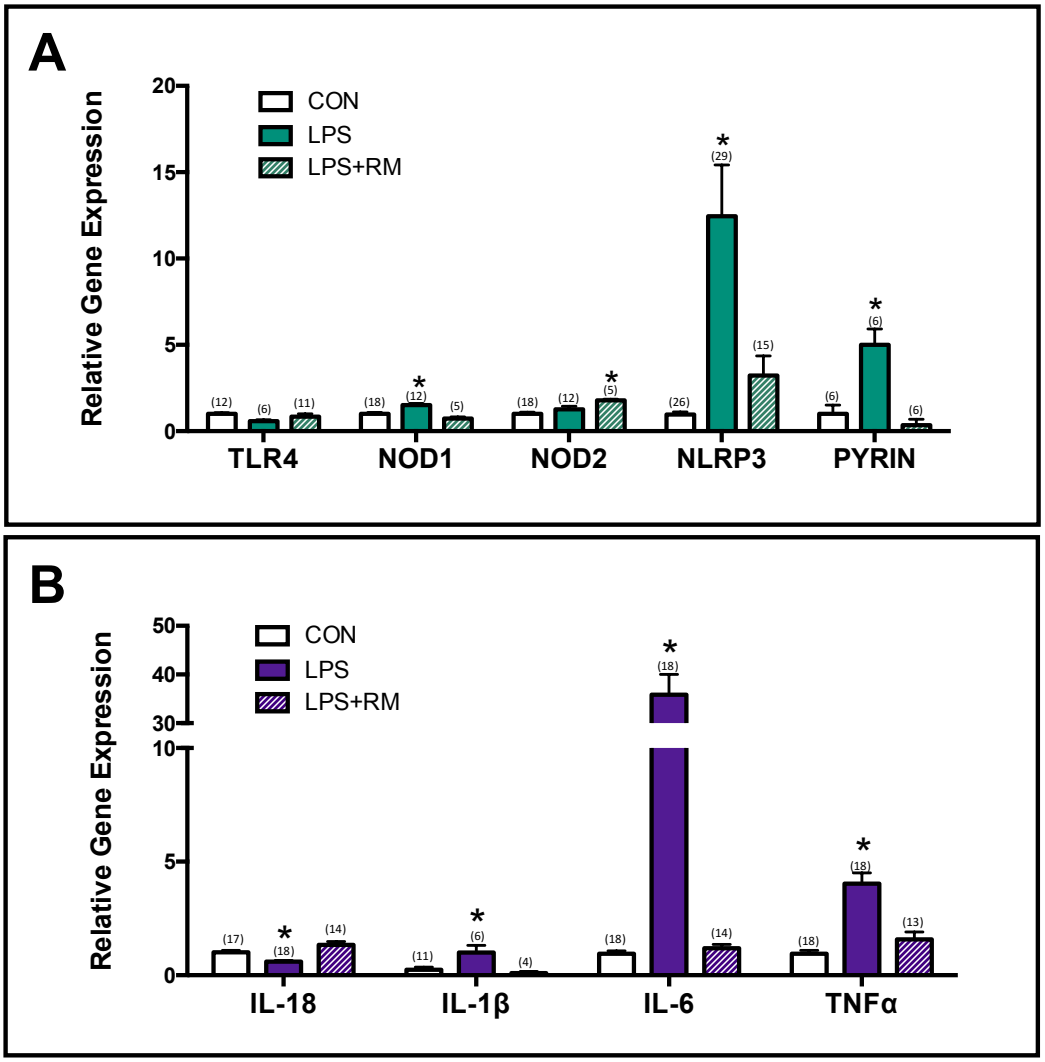

Figure 6| LPS treatment can prime the inflammasome in C2C12 myotubes.

Quantification of the relative changes in gene expression of (A) pathogen recognition receptors (PRR) and (B) pro-inflammatory cytokines. Differentiated C2C12 myotubes were left untreated (CON), treated with 100 ng/mL LPS for 4 hours (LPS), or treated with LPS for 4 hours then washed and left untreated for an additional 48 hours before RNA was collected (LPS+RM). (A) LPS treatment for 4 hours significantly increased NLRP3 and pyrin, components of the NLRP3 inflammasome, as well as another PRR, NOD1. (B) LPS treatment also increased IL6, TNFα, and IL1β gene expression. Data expressed are relative to their respective control (CON) untreated conditions. n≥4 with individual n values denoted above each bar. Values are mean ± SEM, *significantly different from the respective untreated controls (white bar) by one-way ANOVA.

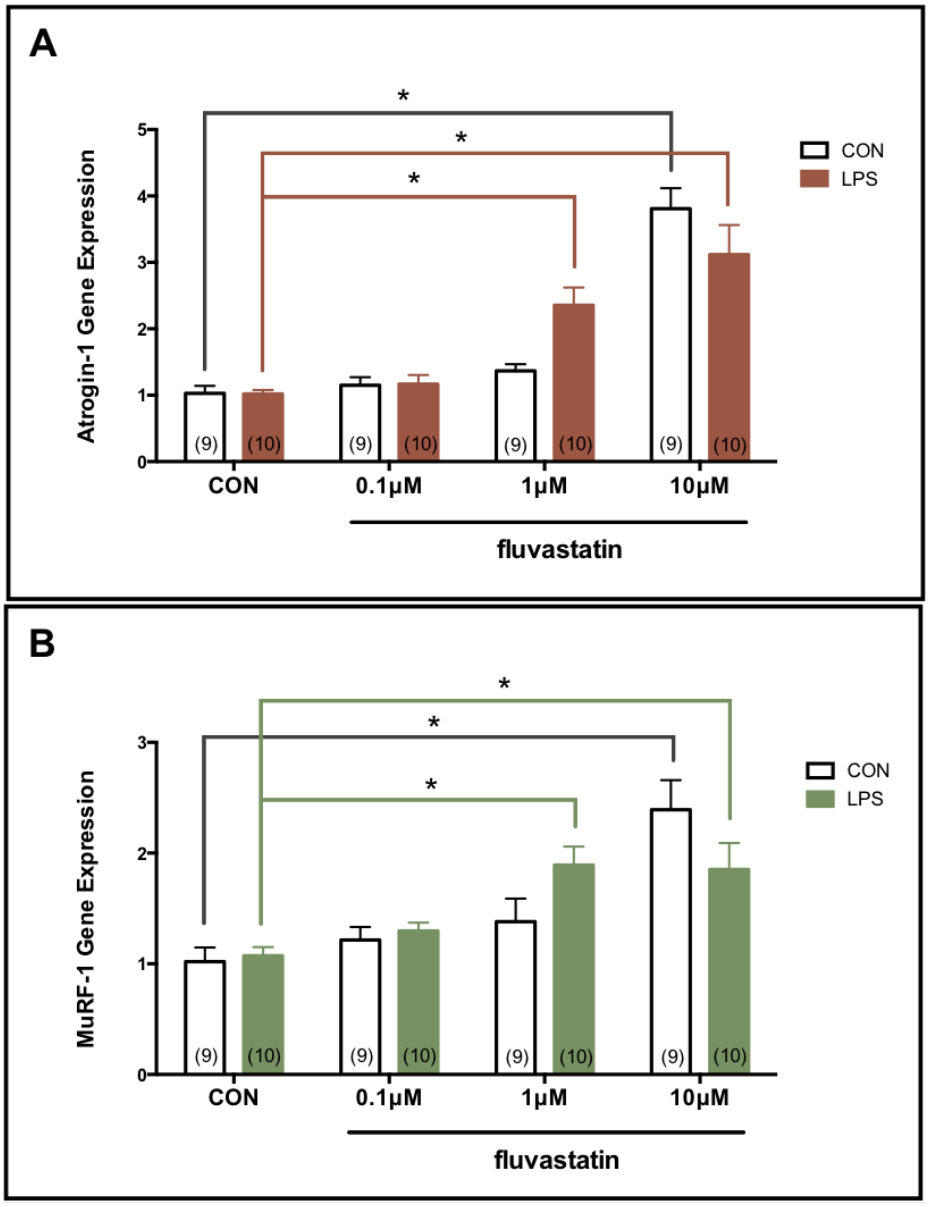

Figure 7| LPS priming decreases the dose of fluvastatin required to increase atrogene expression in C2C12 myotubes.

Gene expression of atrogin-1 (A) and MuRF-1 (B) in C2C12 cells with LPS (100 ng/mL)(LPS) or without LPS (CON) pretreatment before subsequent treatment with fluvastatin (0.1, 1, 10 μM) for 48 hours. 10 μM fluvastatin significantly increases both atrogin-1 and MuRF-1 gene expression, but 1 μM fluvastatin can increase expression only in LPS pretreated cells (red and green bars). All values are relative to respective averaged controls. n≥9 with individual n values denoted inside each bar. Values are mean ± SEM, *significantly different as indicated by the connecting bars by two-way ANOVA.

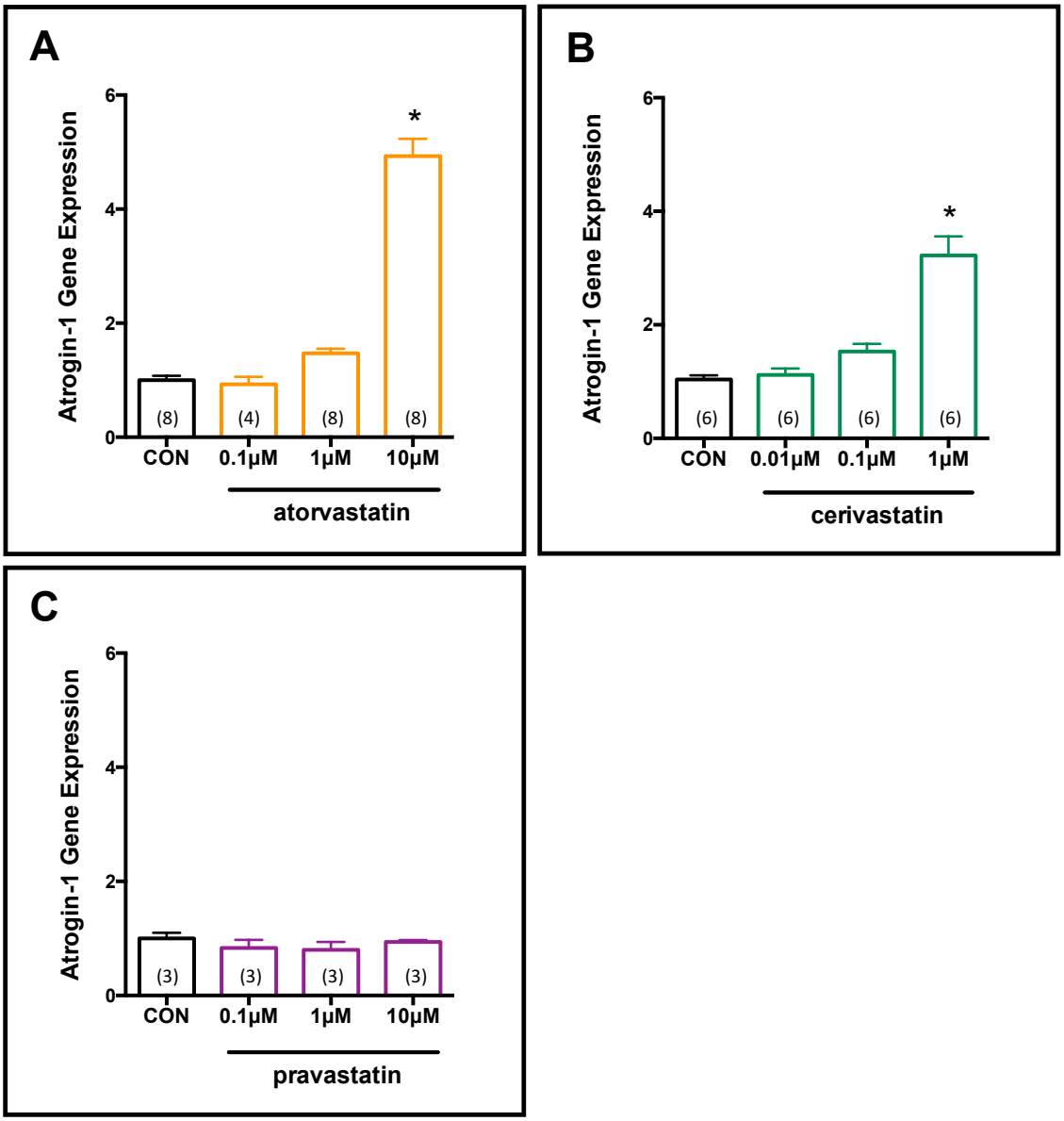

Figure 8| Several, but not all statins increase atrogenes in LPS-primed C2C12 myotubes.

cDNA isolated from atorvastatin, cerivastatin, or pravastatin treated C2C12 myotubes at various doses were measured by RT-PCR. All cells were pretreated with LPS prior to statin treatment. Both atorvastatin (A) and cerivastatin (B) significantly increased atrogin-1 expression. However, pravastatin treatment (C) did not affect atrogin-1 expression in C2C12 myotubes. All values are relative to the average of the respective untreated control (white bar). n≥3. Values are mean ± SEM, *significantly different from untreated control by one-way ANOVA.

4.2 Fluvastatin-treated myotubes have lower Akt/FOXO signaling, which can be overcome with exogenous IGF1

Activation of the PI3K/Akt/FOXO pathway suppresses atrogene transcription. Hence, we determined whether reduced phosphorylation of Akt and FOXO corresponded with the increased atrogene expression in fluvastatin-treated myotubes. Akt regulates FOXO phosphorylation through the partitioning of this transcriptional regulator between the cytosol and nucleus[78]. Specifically, increased phosphorylation of Akt promotes phosphorylation of FOXO, which excludes these transcription factors from the nucleus thereby reducing expression of their targets genes. Regulation of both atrogin-1 and MuRF-1 gene expression can be controlled by phosphorylation of the FOXO family member FOXO3a[90,100]. Akt has been shown to phosphorylate FOXO3a at Thr32, one of its key regulatory sites[101,102].

First, the results showed that fluvastatin treatment of LPS-primed C2C12 cells caused a significant decrease in FOXO3a phosphorylation (Figure 9A). It was also found that fluvastatin (1 μM) significantly lowered Akt phosphorylation at both serine 473 (Ser473) and threonine 308 (Thr308) (Figure 9B, 9C). Akt phosphorylation at Ser473 and at Thr308 was measured in fluvastatin-treated myotubes stimulated with LONG R^3 IGF1 for 30 minutes. We found that exogenous IGF1 resulted in a dose-dependent increase in Akt phosphorylation (Figure 9B, 9C). A low dose of IGF1 (0.1 nM) did not overcome the ability of fluvastatin to decrease Ser473 Akt phosphorylation in C2C12 myotubes (Figure 9B). However, a higher dose of IGF1 (1 nM) eliminated any effect of fluvastatin on Akt phosphorylation (Figure 9B,9C).

We next investigated whether decreased phosphorylation of Akt was reflected in atrogene expression. C2C12 myotubes were treated with 0.1 or 1 nM IGF1 in the presence or absence of fluvastatin (1 μM). As shown previously, fluvastatin significantly increases atrogin-1 and MuRF-1 gene expression following a 48-hour treatment in the absence of exogenous IGF1. A longer period of IGF1 treatment was used to study changes in gene expression, as opposed to changes in acute protein phosphorylation events. A 48-hour IGF1 treatment at doses of 0.1 nM and 1 nM significantly blunted atrogene expression compared to the untreated (i.e. no fluvastatin) control (Figure 9D, 9E). Fluvastatin-induced atrogene expression was significantly reduced by 0.1 and 1 nM IGF1 (Figure 9D, 9E). However, 0.1 nM IGF1 was unable to decrease atrogene gene expression to levels observed with 0.1 nM IGF1-only treatment (Figure 9D, 9E). These data are consistent with a model where fluvastatin-induced decreases in Akt/FOXO3a phosphorylation are linked to the induction of atrogenes, but high doses of IGF1 can overcome fluvastatin's effects on Akt/FOXO3a regulation of atrogene expression.

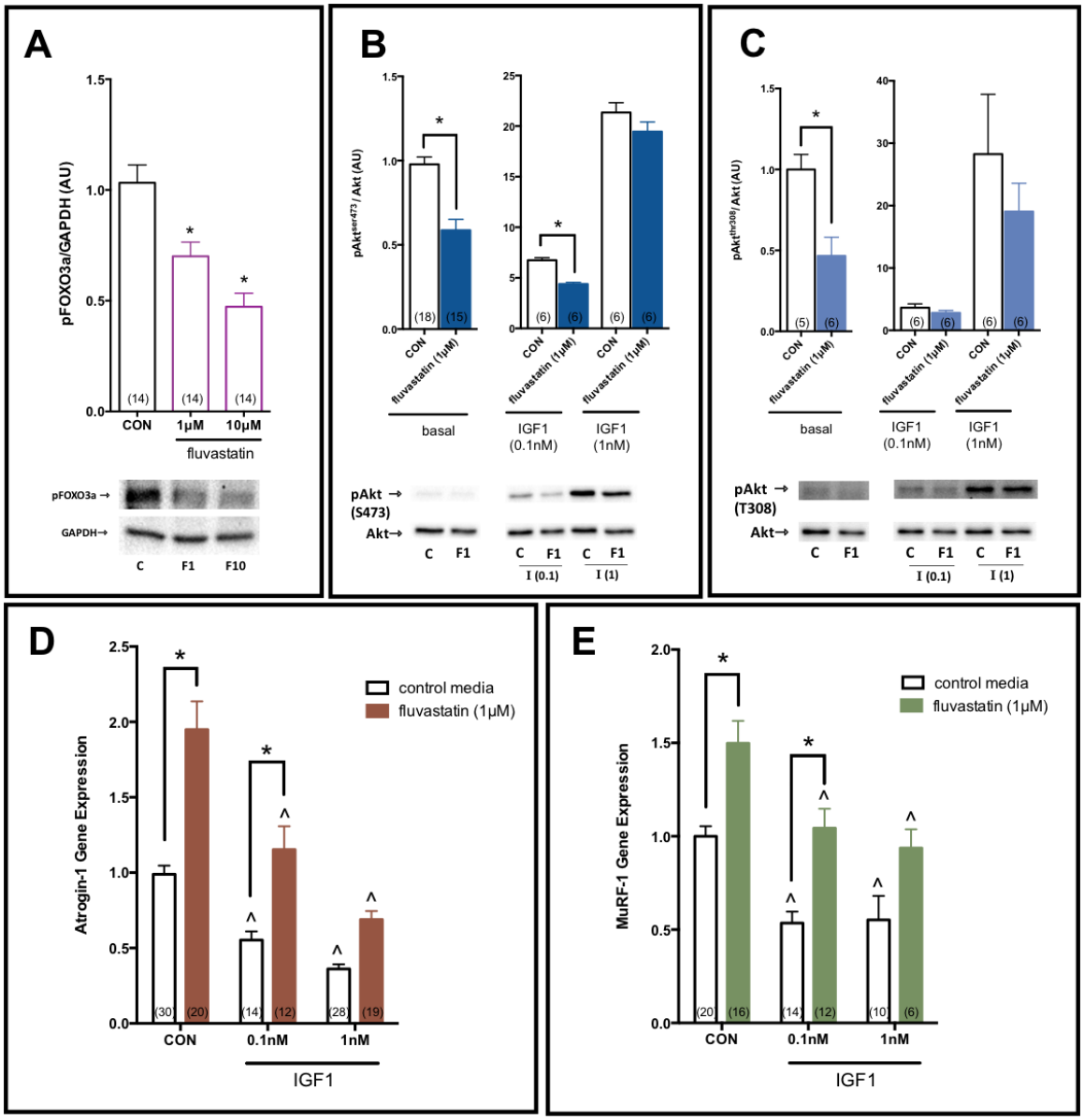

Figure 9| Fluvastatin impairs Akt/FOXO signaling in C2C12 myotubes, which can be overcome by exogenous IGF1.

(A) Protein isolated from LPS-primed, fluvastatin-treated myotubes show a dose-dependent decrease in phospho-FOXO3a (pFOXO3a); *significantly different from untreated control (white bar). Basal phospho-Akt (pAkt) (Ser473) (B) and (Thr308) (C) were significantly decreased in fluvastatin (1 μM)-treated myotubes. In myotubes stimulated with IGF1 for 30 minutes after the 48-hour fluvastatin treatment protocol, a low and high dose of IGF1 are both able to increase pAkt (B and C). However, pAkt (Ser473) remains blunted in fluvastatin-treated cells stimulated with a low dose (0.1 nM) of IGF1.

Observed effects in Akt phosphorylation correlate well with atrogin-1 expression in myotubes co-treated with fluvastatin (1 µM) and IGF1 for 48 hours. IGF1 significantly suppresses atrogin-1 (D) and MuRF-1 (E) gene expression compared to the untreated control (CON white bar). Additionally, IGF1 can partially suppress the fluvastatin-induced increase in atrogene expression; ^significantly different from the respective controls (CON white bar or CON red/green bar). For representative blots below each graph, C=control, F1=fluvastatin (1 µM), F10=fluvastatin (10 µM), I=IGF1 (0.1 or 1nM as indicated). All values are relative to respective averaged control conditions. n≥6 for protein data and n≥16 for gene expression data. Values are mean ± SEM, *significantly different from untreated control and as indicated by connecting bars by Student's T-Test for pAkt analysis, and by two-way ANOVA for atrogin-1 and MuRF-1 expression analysis.

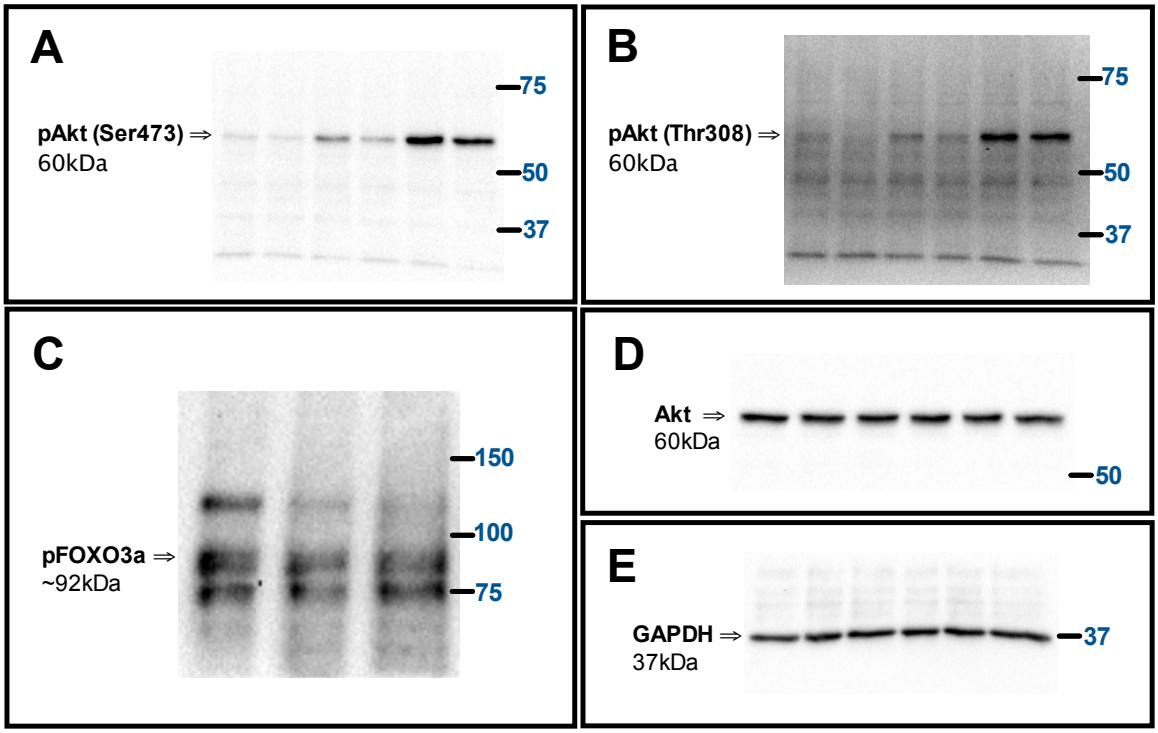

Figure 10| Representative blots.

Example immunoblots for all antibodies tested (A-E). Numbers listed to the right of each image indicates the estimated molecular weights as determined based on the protein ladder.

4.3 Restoring isoprenoids, but not cholesterol, prevents fluvastatin-induced atrophy and atrogin-1 in muscle cells

To further investigate the mechanisms that contribute to fluvastatin-induced myopathy in C2C12 myotubes, we next determined if isoprenoid or cholesterol intermediates of the mevalonate pathway mediate changes in atrogene expression. C2C12 myotubes were treated with fluvastatin in the presence or absence of geranylgeranyl pyrophosphate (GGPP, 10 μM) or 25-hydroxycholesterol (25HC, 10 μM) for 48 hours. As expected, atrogin-1 was increased in myotubes treated with fluvastatin, but co-treatment with 10 μM of GGPP significantly lowered atrogin-1 expression (Figure 11A). Interestingly, co-treatment with 25HC significantly potentiated the fluvastatin-induced atrogin-1 gene expression (Figure 11A). This effect was also seen by measuring the diameters of myotubes. Myotubes exposed to GGPP and fluvastatin had larger diameters compared to fluvastatin exposure alone (Figure 11B, 11C). In contrast, Myotubes exposed to both 25HC and fluvastatin had significantly smaller diameters when compared to the fluvastatin-only treatment (Figure 11B, 11C).

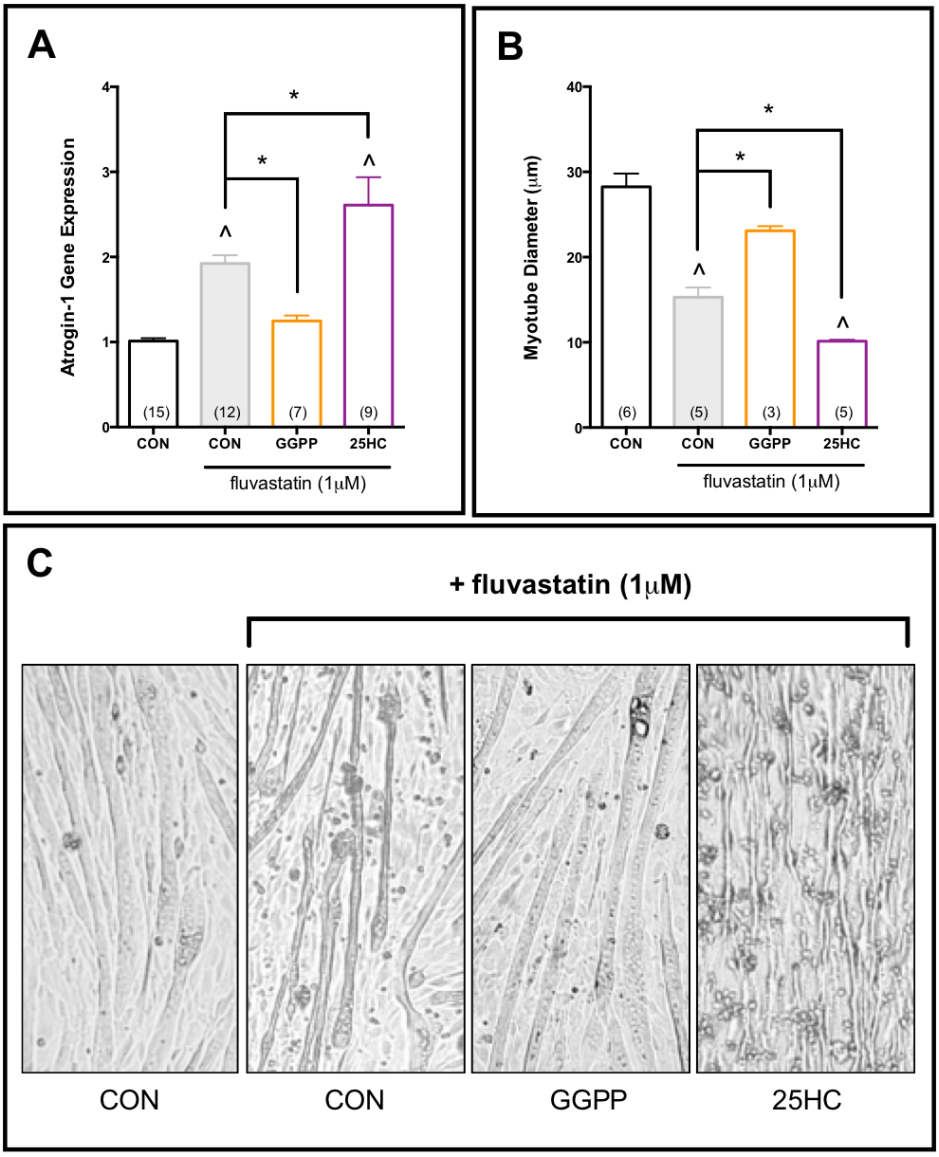

Figure 11| Decreased prenylation is required for fluvastatin-mediated atrophy and increased atrogin-1 expression.

LPS primed, fluvastatin (1 μM)-treated myotubes were co-treated for 48 hours with 10 μM geranylgeranyl pyrophosphate (GGPP) or 10 μM 25-hydroxycholesterol (25HC). (A) GGPP significantly decreased atrogin-1 expression, whereas 25HC (B) potentiated atrogin-1 expression. (C) This effect could be visualized in images taken by light microscopy, and quantification of myotube diameters (B) correlates with atrogin-1 gene expression data. Values are mean ± SEM, n≥7 for gene expression data, n≥3 for myotube diameter quantification. ^significantly different from untreated control (white bar), *significantly different as indicated by connecting bars by one-way ANOVA.

4.4 Fluvastatin-treated myotubes have increased caspase-1 activity, which is mediated by decreased isoprenoids

We next determined if fluvastatin treatment alters caspase-1 activity, which is a key component of the NLRP3 inflammasome. The amount of active caspase-1 was measured using a FAM-FLICA assay in myotubes treated in the presence and absence of fluvastatin with and without LPS priming. We found that the combination of LPS priming and fluvastatin (1 μM) treatment caused significantly higher levels of active caspase-1 compared to both primed and unprimed myotubes that were not exposed to fluvastatin (Figure 12A). This result was further confirmed with a different caspase-1 activity assay that measures the cleavage of the caspase-1 substrate YVAD in C2C12 myotube lysates. Similar to the FAM-FLICA assay results, these results showed that fluvastatin treatment resulted in a dose-dependent increase in caspase-1 activity in LPS primed C2C12 myotubes (Figure 12B). We next determined if protein prenylation can regulate caspase-1 activity. The results showed that providing the isoprenoid GGPP (10 μM) decreased the amount of active caspase-1 in myotubes treated with 10 μM fluvastatin (Figure 12C).

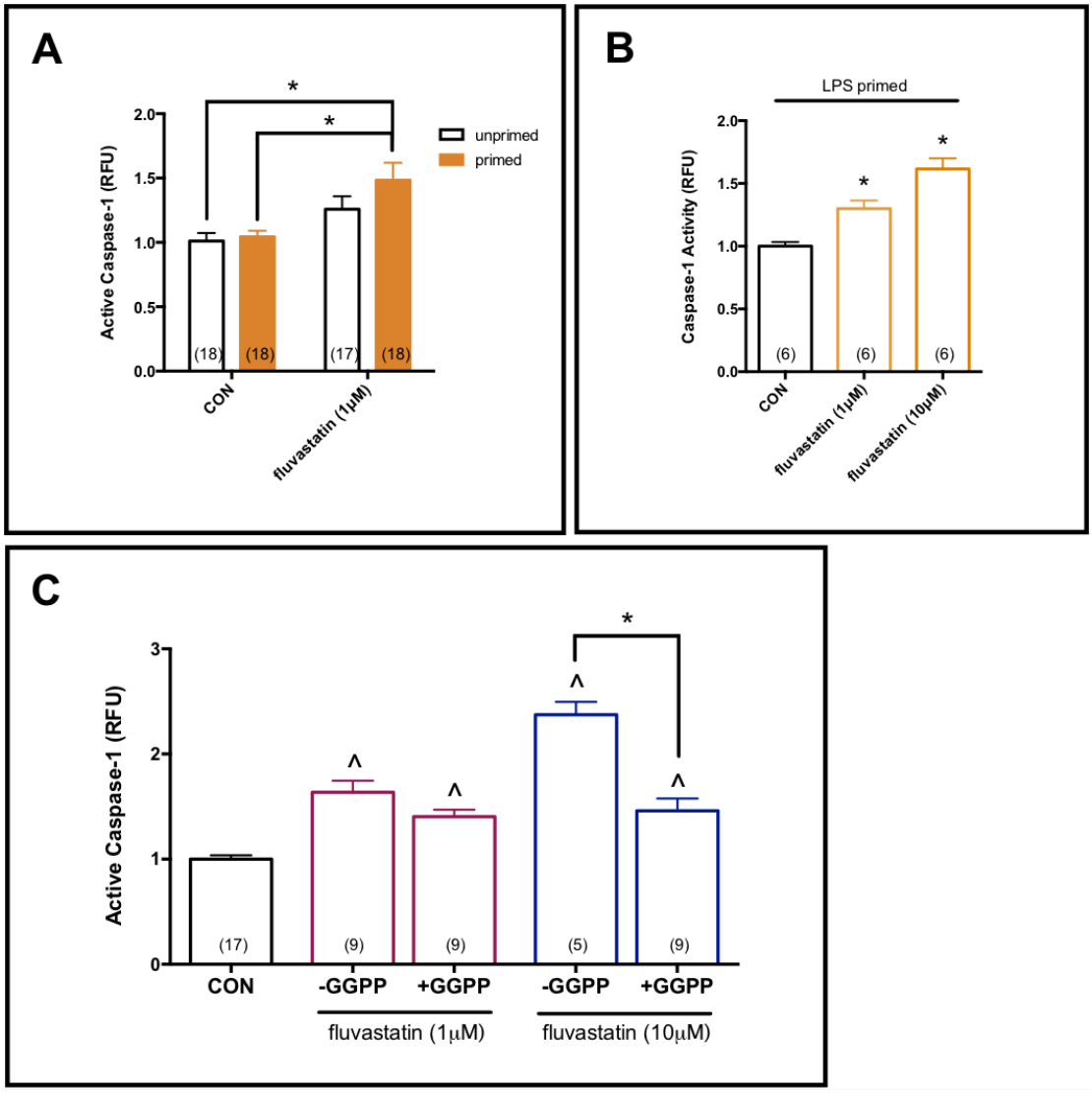

Figure 12| Increased caspase-1 activity in fluvastatin-treated myotubes is mediated by decreased prenylation.

(A) Myotubes, LPS-primed or unprimed, were treated with fluvastatin (1 μM) for 48 hours. Treatment media was then removed and FLICA solution was added. Active caspase-1 measured as relative fluorescence intensity, was significantly increased only in LPS-primed cells. (B) Caspase-1 activity increases in a dose dependent manner in LPS primed cells treated with fluvastatin (1 μM and 10 μM) for 48 hours. (C) Increased active caspase-1 is rescued by GGPP (10 μM) in myotubes treated with fluvastatin (10 μM). Values are mean ± SEM, n≥6 for all conditions, ^*significantly different from untreated controls (white bar) or as indicated by connecting bars, by two-way (A) or one-way ANOVA (B and C).

4.5 Inhibitors of the NLRP3 inflammasome and caspase-1 attenuate fluvastatin-induced atrogin-1 in myotubes

We next determined if chemical or peptide-based inhibitors of the NLRP3 inflammasome or various caspases regulate atrogene expression during fluvastatin treatment in C2C12 myotubes. Two peptide-based caspase-1 inhibitors were used: the pan-caspase inhibitor Z-VAD-FMK and the caspase-1 inhibitor Z-WEHD-FMK, and NLRP3 inflammasome inhibition was achieved using the glyburide derivative Z56765797 (3-chloro-N-(5-chloro-2-methoxyphenyl)-4-methoxybenzamide) which blocks the ATP/K^+ activation of the NLRP3 inflammasome. All of these inhibitors significantly lowered atrogin-1 gene expression in myotubes treated with 1 μM or 10 μM fluvastatin, compared to fluvastatin treatment alone (Figure 13A, 13B, 13C).

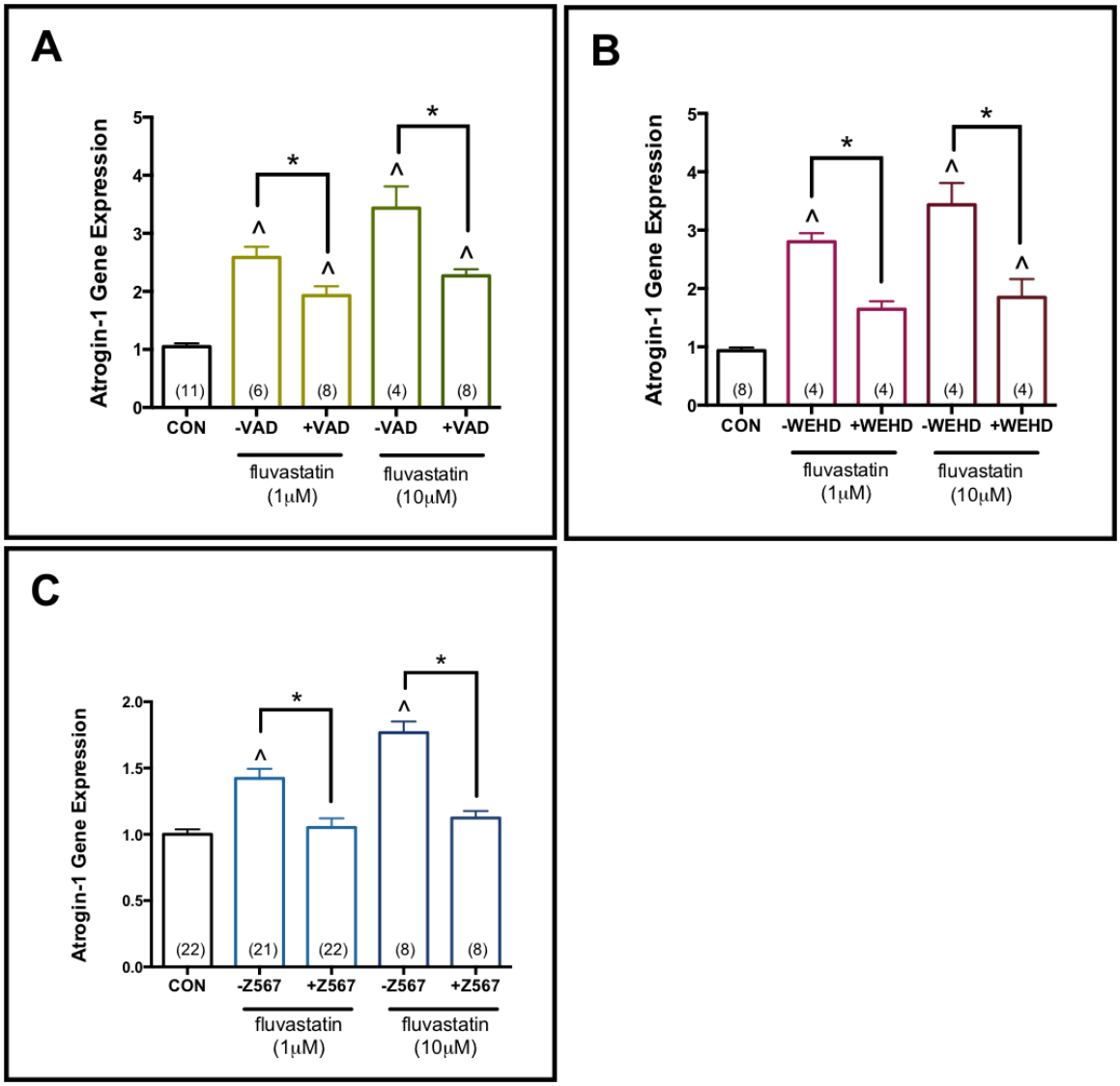

Figure 13| Inhibitors of caspase-1 and NLRP3 rescue fluvastatin-mediated increases in atrogin-1.

LPS-primed myotubes were co-treated with 10 µM pan-caspase inhibitor Z-VAD-FMK (VAD), 10 µM caspase-1 inhibitor Z-WEHD-FMK (WEHD), or 50 µM NLRP3 inflammasome inhibitor Z56765797 (Z567) and 1µM fluvastatin for 48 hours before RNA was collected. Analysis of gene expression shows caspase-1 inhibitors (A and B) can prevent fluvastatin-induced atrogin-1 expression. A similar effect was also observed with the NLRP3 inhibitor (C). Values are mean ± SEM, n≥4 for all conditions, ^significantly different from the untreated control (white bar), *significantly different as indicated by the connecting bars, by one-way ANOVA.

4.6 GGPP can rescue FOXO3a signaling in fluvastatin treated myotubes

The rescue effect of GGPP and inhibitors of caspase-1 and NLRP3 on atrogin-1 expression may be indicative of improved Akt signaling as atrogenes can be regulated through decreased activity of this signaling pathway[92,103]. Fluvastatin decreased Ser473 Akt phosphorylation, but caspase-1 and NLRP3 inhibitors did not increase Akt phosphorylation (Ser473) signaling (Figure 14A). Exogenous GGPP had a small effect on Akt phosphorylation (Ser473) since it prevented a statistically significant decline due to fluvastatin. However, further investigation showed that GGPP is able to significantly increase FOXO3a phosphorylation (Figure 14B), which provides evidence that restoring prenylation alters FOXO3a regulation of atrogene expression.

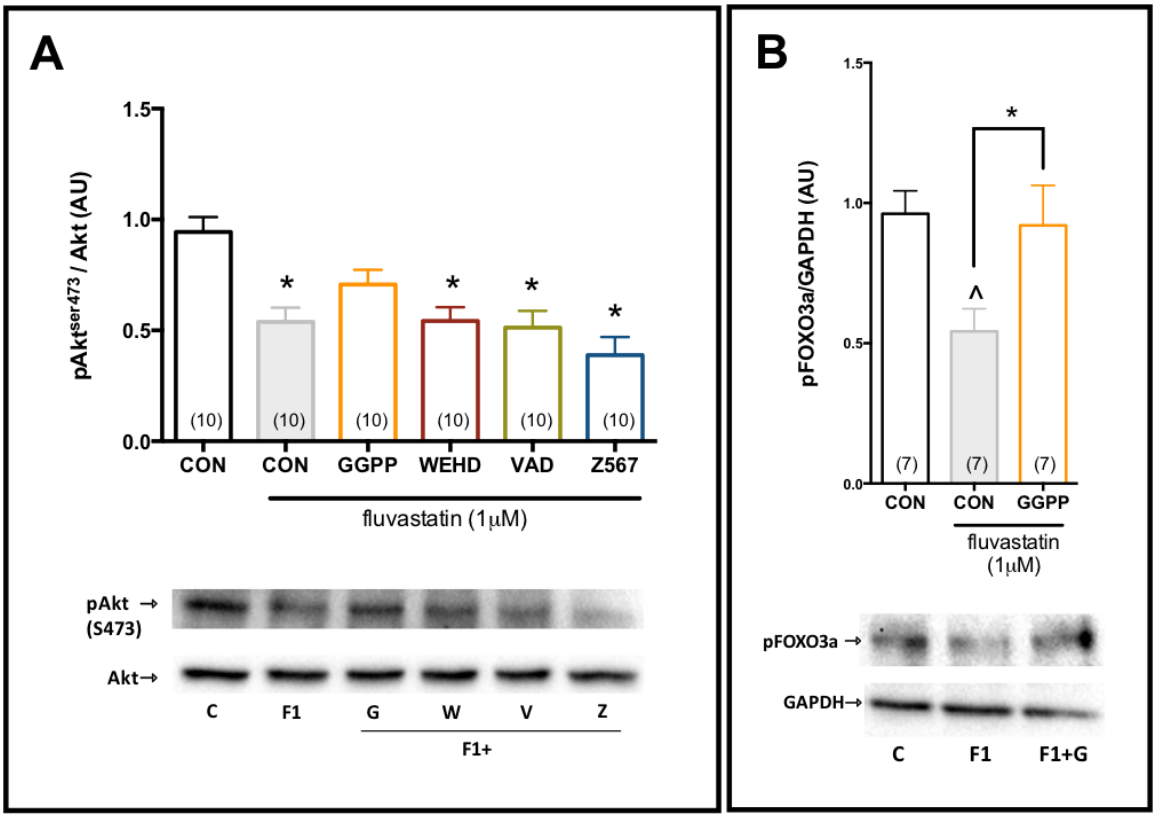

Figure 14| GGPP treatment rescues fluvastatin mediated defects in FOXO3a phosphorylation.

Protein was collected from LPS-primed, 48-hour fluvastatin (1 μM) and GGPP (10 μM) co-treated myotubes. (A) pAkt (Ser473) was not significantly rescued by GGPP, however (B) pFOXO3a was. Values are mean ± SEM, n≥6 for all conditions, ^significantly different from the untreated control (white bar), *significantly different as indicated by the connecting bars, by one-way ANOVA.

5.0 DISCUSSION

The mechanisms contributing to statin-induced myopathy remain ill-defined. Statins are widely used because of their proven effectiveness in lowering cholesterol and risk reduction of cardiovascular events. Muscle toxicity is the most commonly recognized side effect of statins[57], and can also be one of the most serious side effects as rhabdomyolysis can be fatal[53]. However, the majority of statin-induced side effects on skeletal muscle are related to muscle pain, exercise intolerance, and weakness[61,104,105]. There is no established cell culture or animal model that captures the spectrum of these various severities of statins on muscle. Furthermore, it is not known if the mechanisms underlying rhabdomyolysis are common to less severe forms of statin myopathy. Therefore, the purpose of this thesis was to investigate if a specific inflammatory pathway was linked to markers of statin myopathy, using a cell culture model that was less severe than overt rhabdomyolysis. We sought to provide insight into a pathway that could contribute to aspects of statin myopathy without comprising the cardiovascular benefits of this drug class.

We aimed to understand if statins engaged a specific inflammatory pathway and contributed to a gene program involved in muscle cell atrophy, independently of cholesterol-lowering pathways. Generally, statins have been associated with having anti-inflammatory effects, and this is thought to confer some of the cardiovascular benefits. However, recent evidence from *in vitro* and clinical studies have shown that statins can also generate a specific pro-inflammatory response in immune cells via activation of the

NLRP3 inflammasome. We sought to investigate the role of the NLRP3 inflammasome in aspects of statin-induced myopathy using an *in vitro* muscle cell autonomous model. Statins alone are already known to increase atrophy-related genes (ie. atrogenes), which are markers of myopathy in C2C12 muscle cells. However, previous *in vitro* models have used high statin doses between 10-100 μM of fluvastatin, which are typically higher than those achieved in the circulation of statin patients[106,107].

An effective NLRP3 inflammasome response generally involves two steps, namely priming and activation. We found that the commonly used priming agent LPS, could prime the NLRP3 inflammasome and that statins could activate this inflammasome in muscle cells. Importantly, we provided evidence that priming the NLRP3 inflammasome with LPS in C2C12 myotubes lowered the dose of fluvastatin required to increase markers of myopathy (i.e. atrogenes) by at least 10-fold.

We showed for the first time that fluvastatin increased muscle cell caspase-1 activity in an isoprenoid-dependent manner. The isoprenoid arm of the mevalonate pathway is independent of the biosynthesis of cholesterol, but still mediated by the primary target of statins, HMG-CoA reductase. Furthermore, we showed that statin-induced atrogene induction was not due to changes in a specific cholesterol intermediate (25HC), but coincided with decreased FOXO3a phosphorylation. In addition, we discovered that inhibitors of caspase-1 and NLRP3 prevented statin-induced atrogene expression in muscle cells. These findings are consistent with a model where statins lower protein prenylation and activate the NLRP3/caspase-1 inflammasome, which may

increase muscle atrogene expression through inhibition of the Akt/FOXO pathway. This is important because this potential mechanism of statin-induced muscle myopathy is independent of the cholesterol-lowering effect of statins, and therefore has the potential to be targeted separately from the cholesterol-lowering statin effects through combinational drug therapy.

5.1 Priming the NLRP3 inflammasome reduces the dose of fluvastatin required to induce atrogenes

Previous studies have explored the importance of atrogenes in statin-induced myopathy. Hanai et al. provided the first evidence that induction of the muscle-specific E3 ubiquitin ligase atrogin-1 is necessary for the muscle damage observed in lovastatin treated C2C12 myotubes and zebrafish[88]. In addition, they showed that statin patients with symptomatic myopathy expressed higher levels of atrogin-1 in quadricep biopsies. Elevated atrogene expression (atrogin-1 and MuRF-1) has also been observed in various mouse models of statin myopathy[87,108]. In accordance with this previous work, we have shown that fluvastatin, atorvastatin, and cerivastatin increase atrogin-1 expression in C2C12 myotubes. Interestingly, we found that pravastatin did not increase atrogin-1 expression even at a high dose (10 μM). In ranked order from most to least, cerivastatin, fluvastatin, and atorvastatin are considered to be hydrophobic statins, while pravastatin is recognized as a hydrophilic statin[109]. This may be one factor in discordant muscle myopathy because the transport of pravastatin across the cell membrane requires an organic anion transporter polypeptide (OATP). In mice, uptake of pravastatin is primarily

mediated by OATP1A4, which C2C12 cells do not express to an appreciable amount[110,111]. In humans, the PRIMO clinical study found that the most hydrophilic statins (pravastatin) were the least likely to cause myalgia, while lipophilic statins (atorvastatin, simvastatin) were associated more with muscular adverse events[52]. Moreover, cerivastatin, the most hydrophobic statin, was removed from market for having an unacceptably high rate of rhabdomyolysis[112].

For the first time, we have also shown that C2C12 myotubes are more sensitive to a lower dose of fluvastatin when myotubes are first primed with LPS. In immune cells, LPS is an established priming agent for the NLRP3 inflammasome. As mentioned before, this cytosolic immune receptor usually requires two steps to generate a caspase-1 response. In most cases, priming of the NLRP3 inflammasome facilitates activation by a variety of endogenous and exogenous stimuli. However, in certain cells caspase-1 activity is uncoupled from a two-step process of pathogen and danger signal detection. For example, macrophages, but not monocytes require priming and an activating signal to increase caspase-1[113]. In addition, alternate inflammasome activation that requires only a single stimulus (such as a TLR4 ligand) can occur in certain monocytes[114]. Our results demonstrate that mouse muscle cells show responses indicative of the canonical, two-step NLRP3 inflammasome. Our results on the effects of priming on atrogene expression are some of the first evidence showing that muscle cells increase NLRP3 transcript levels in response to NLRP3 priming stimuli. We also show that this has an effect on activation of the inflammasome (discussed below). Hence, we have found that C2C12 muscle cells

can mount a cell autonomous NLRP3 inflammasome response to statins, and at least one of the effects of this muscle cell immune response is increased atrogene expression.

5.2 Prenylation mediates statin-induced caspase-1 activity in C2C12 myotubes

Fluvastatin treatment dose-dependently increased caspase-1 activity in muscle cells. Caspase-1 is the key effector component of the NLRP3 inflammasome[42]. Fluvastatin has also been shown to stimulate caspase-1 activity in peripheral blood mononuclear cells[24], and more recently, fluvastatin was shown to increase caspase-1 activity in adipose tissue[98]. This effect on caspase-1 activity does not appear to be limited to fluvastatin as simvastatin has also been found to stimulate caspase-1 mediated processing of pro-IL-1β in THP1 monocytes[115]. We did not test if multiple statins activate caspase-1 in muscle cells. However, we would expect that this effect is not specific to fluvastatin, since we showed that multiple statins increased atrogene expression in LPS primed muscle cells. It has been shown that statins promote atrogene induction by inhibiting the synthesis of isoprenoids like GGPP[89,116]. Moreover, reduced prenylation also mediates statin induced caspase-1 activity in immune cells[117,118]. Putting these two concepts together, we found that statin-induced caspase-1 activity can be regulated by GGPP in myotubes. Specifically, LPS-primed myotubes treated with both fluvastatin and GGPP had significantly lower levels of active caspase-1 when compared to myotubes treated with only fluvastatin. These results are important because they show a muscle cell autonomous inflammasome/caspase-1 response due to statins that is prenylation-dependent. Caspase-1 activation is primarily dependent on formation of the NLRP3 inflammasome, therefore our results show that

statins activate the NLRP3 inflammasome in a way that depends on depletion of isoprenoids required for protein prenylation, specifically GGPP. This suggests that reduced protein prenylation is upstream of the NLRP3 inflammasome in response to statins. This thesis did not identify the specific prenylated proteins that alter NLRP3 inflammasome activity, but future experiments will try to investigate these affected proteins.

5.3 Inhibitors of NLRP3 and caspase-1 lower fluvastatin-induced atrogene expression

We demonstrated that: 1) statin-reduced prenylation activated caspase-1 and 2) reduced prenylation is required for statin-induced atrogene expression. Hence, we next tested if blocking NLRP3 and caspase-1 altered statin-induced atrogene responses in muscle cells.

We first confirmed that providing exogenous GGPP prevented statin-induced atrogene expression in muscle cells. Our results showing that restoring the isoprenoid required for protein prenylation prevents statin-induced atrogene expression is consistent with previous reports[89]. We also showed that both pan-caspase and caspase-1 inhibitors (Z-VAD-FMK and Z-WEHD-FMK) and the NLRP3 inflammasome inhibitor, Z56765797 (a glyburide derivative), all prevented the increased atrogin-1 expression caused by fluvastatin treatment in muscle cells. Our results are consistent with a model where statins lower prenylation, which activates the NLRP3/caspase-1 inflammasome, which is then required to increase muscle atrogenes.

Additionally, we have ruled out a specific cholesterol intermediate in these statin-induced effects on atrogenes. This was important for several reasons. First, it has been

shown that levels of the cholesterol intermediate we tested, 25HC, and total cellular cholesterol are directly related. More importantly, 25HC was recently found to regulate inflammasome activity during viral infections. Reboldi et al. showed that decreased cellular content of 25HC leads to increased caspase-1 activity and increased IL-1β in macrophages[119]. As statins significantly inhibit cholesterol biosynthesis, we would expect a similar drop in 25HC levels, which could then activate the NLRP3 inflammasome. However, our results suggest that statin-induced reductions in 25HC is not a mediator of increased NLRP3/caspase-1 inflammasome activity in C2C12 muscle cells. Our results actually show that providing exogenous 25HC can synergize with fluvastatin to further increase atrogin-1 expression. Therefore, these results are consistent with a model where 25HC synergizes or amplifies inflammatory signals outside of the NLRP3 inflammasome, as demonstrated by others[120].

5.4 Exogenous IGF1 can overcome fluvastatin-mediated suppression of Akt/FOXO signaling in muscle cells

It was recently shown that statin-mediated activation of the NLRP3 inflammasome promotes insulin resistance in adipose tissue[98]. Many aspects of insulin and IGF1 signaling are conserved, including stress kinase and inflammatory suppression of Akt signaling downstream of insulin/IGF1 receptors[121]. Similar to statin-mediated insulin resistance in adipose tissue, we investigated if statins promoted IGF1 resistance or altered Akt signaling in muscle cells. In skeletal muscle, the phosphorylation status of Akt controls FOXO3a, which has been shown to be a master regulator of atrogene expression. When Akt is

dephosphorylated, FOXO3a also remains dephosphorylated, causing localization in the nucleus, thereby increasing atrogin-1 and MuRF-1 transcription and increasing ubiquitin-proteasome-mediated proteolysis[92]. We first assessed this phosphorylation cascade in the absence of IGF1 (i.e. basal conditions). As expected, we saw a dose-dependent decrease in FOXO3a phosphorylation with increasing doses of fluvastatin in LPS primed muscle cells. In addition, we saw reduced basal phosphorylation of Akt at both Ser473 and Thr308. This is consistent with data presented by Mallinson et al. which showed lower Akt (Ser473)/FOXO3a signaling in an *in vivo* mouse model of statin myopathy using simvastatin[87].

However, we have also demonstrated that exogenous IGF1 is able to rescue the fluvastatin-mediated increase in atrogin-1 as well as increase Akt phosphorylation in statin-treated myotubes. This would suggest that fluvastatin-treated myotubes with lower basal Akt/FOXO signaling are still responsive to exogenous activators of Akt signaling. Interestingly, at a low dose of IGF1 (0.1 nM) Akt phosphorylation of Ser473 was not as robust in fluvastatin treated myotubes. However, basal defects in Akt phosphorylation at Thr308 were lost with IGF1 treatment. Phosphorylation of Thr308 by PDK1 imparts only partial activation of the IGF1/PI3K/Akt pathway[122]. However, partial activation is sufficient to activate mTORC1, whose substrates include proteins involved in protein synthesis (4EBP1 and S6K1). Phosphorylation of Akt at Ser473 by mTOR in the IGF1/PI3K/Akt pathway stimulates full Akt activity that leads to additional substrate-specific phosphorylation events in both the cytoplasm and nucleus[123]. Importantly, fully

active Akt mediates the phosphorylation of FOXO transcription factors regulating protein degradation. Therefore, restored signaling in fluvastatin treated myotubes stimulated with IGF1 (0.1 nM), implies the protein synthesis arm is restored. Conversely, defects in Ser473 Akt phosphorylation remain with IGF1 (0.1 nM) stimulation suggesting continued impairment of the protein degradation arm and elevated atrogene transcription.

Importantly, our results showed that providing exogenous GGPP restored FOXO3a phosphorylation during fluvastatin treatment levels equivalent to control, untreated muscle cells. This provides direct evidence that GGPP rescues atrogin-1 expression with fluvastatin treatment in an Akt/FOXO signaling-dependent manner. The effect of GGPP on Ser473 phosphorylation of Akt are less clear, but prenylation may also be involved in the regulation of statin-induced changes in Akt phosphorylation, as there appears to be a trend for an increase in Akt phosphorylation when GGPP is provided with fluvastatin treatment. In contrast with our results, Ogura et al. showed that reduced Akt phosphorylation in simvastatin-treated C2C12 myotubes could not be rescued by GGPP, or the other isoprenoid intermediate FPP and mevalonate[124]. However, this was observed under exogenous IGF1 stimulating conditions, which could have masked any effects of rescue in Akt phosphorylation given the substantial increase in Akt phosphorylation quantified in cells stimulated with a very high dose of IGF1 (50 nM). Additionally, we saw a more robust rescue in FOXO3a phosphorylation rather than Akt phosphorylation, which provides more direct evidence for the importance of this pathway in regulating atrogenes.

5.5 LIMITATIONS

In our model of statin-induced myopathy, LPS was used as a priming signal for the NLRP3 inflammasome. However, an LPS dose of 100 ng/mL is significantly greater than levels achievable in adult humans. Even patients experiencing life-threatening septic shock are reported to have circulating levels of LPS only in the range of 700 pg/mL[125]. In healthy adults, serum LPS levels are even lower and may only be as high as 1.5 pg/mL[126]. Although our choice of LPS dose may not be clinically relevant, it was chosen based on established cell-based models of inflammasome priming[115,127,128]. It is also important to mention that LPS does not represent the sole priming signal, as many pro-inflammatory cytokines can also activate NFκB to prime the NLRP3 inflammasome[129].

Additionally, in our analysis of FOXO3a signaling, phosphorylation of FOXO3a was normalized to the GAPDH loading control instead of total FOXO3a. Therefore, although changes in FOXO3a phosphorylation were observed, it is also possible that total FOXO3a protein content changes with statin treatment. Future experiments will need to test for protein levels of total FOXO3a to correct for this. Furthermore, the majority of the data presented reflect on changes in gene expression and not protein or activity levels. Although changes in atrogene expression have been shown to correlate with protein levels in other studies, it may be worthwhile to confirm the changes in gene expression we observed with protein and activity measures of these muscle-specific E3 ubiquitin ligases to gain further insight into their regulation during statin myopathy.

Using our model of statin myopathy, we showed that atrophy programs are upregulated with fluvastatin treatment. However, in this model, treatment was administered while myotubes were still maturing and differentiating, which may have impacted their fusion and growth. Therefore, although we have shown that fluvastatin treatment induces atrogene expression, it remains to be determined if fluvastatin has negative effects on myoblast fusion and myotube growth in our model.

In general, the applicability of an *in vitro* model of statin-induced myopathy poses some challenges in interpreting and concluding on the generated data. It will be important to test this model of statin-induced myopathy *in vivo* and in human muscle tissue samples, in order to better understand how physiological factors can impact our findings. Importantly, cross-talk between muscle and other cell types like immune cells, may regulate or potentiate statin myopathy effects, as the NLRP3 inflammasome response is most robust in macrophages and monocytes.

5.6 FUTURE DIRECTIONS

Additional work *in vitro* should be conducted to better understand the mechanistic progression of statin-induced myopathy. Specifically, it will be important to understand how NLRP3/caspase-1 activation induces atrogene expression. As observed with GGPP rescue of atrogene expression through restoring FOXO3a phosphorylation, inhibitors of caspase-1 and NLRP3 may have a similar effect on the phosphorylation status of FOXO3a. Protein samples from fluvastatin-treated myotubes co-treated with Z-VAD-FMK, Z-WEHD-FMK or Z56765797 for 48 hours can be used in immunoblotting to probe for changes in

FOXO3a phosphorylation. It is also possible that NLRP3/caspase-1 activation acts downstream of FOXO3a. There is evidence in cardiomyocytes demonstrating that reduced apoptosis repressor with caspase recruitment domain (ARC), a downstream protein of FOXO3a, upregulates caspase-1 and pro-inflammatory cytokines IL-1β and IL-18[130]. Therefore, if ARC is involved in statin myopathy, we would expect silencing ARC using siRNA in LPS-primed C2C12 myotubes to mimic the effects of fluvastatin on inducing atrogene expression. Additionally, atrogene transcription has also been found to be regulated by stress kinases[97]. Activation of the p38 stress kinase can be measured by immunoblotting to determine if statin-mediated atrogene expression is limited to regulation by the Akt/FOXO3a signaling pathway in our model of statin-induced myopathy. Chemical inhibitors of p38 can also be utilized to observe the effects of p38 signaling inhibition on atrogene expression.

As mentioned in limitations, future experiments should also aim to evaluate the effect of statins on myoblast differentiation and fusion to conclusively determine whether statins work primarily to promote atrophy-related programs in muscle cells. This can be done by measuring markers of fusion such as quantifying the number of myotubes with nuclei over a set threshold, or by determining the fusion index by dividing the number of nuclei in myotubes by the total number of nuclei analyzed[131]. In addition, changes in myotube size and number may be indicative of cell death. This is important as other studies have shown that statins can induce apoptosis in a variety of cell types[58,71]. Moreover, activation of caspase-1 can lead to the initiation of inflammatory cell death

(pyroptosis), which is often seen in immune cells[132]. Thus, future experiments will need to be done to measure cell death in our model of statin-induced myopathy. Cell viability/death can be measured with trypan blue exclusion assays, and induction of apoptosis could be measured using caspase-3 activity assays in primed and unprimed C2C12 myotubes treated with 1 μM of fluvastatin. Additionally, caspase-3 specific inhibitors can be utilized to determine if inhibiting apoptosis can also mediate changes in atrogene expression in our model.

To expand the applicability of this work into a clinical setting, it will be important to test this model of statin-myopathy *in vivo*, or *ex vivo*. Using NLRP3 knockout mice ($NLRP3^{-/-}$), fluvastatin chow diet can be administered *ad libitum* for several weeks to mimic treatment protocols in statin patients. Muscle tissue would then be collected to look at markers of myopathy, including cross-sectional area, presence of myopathy, atrogene gene and protein expression, and caspase-1 activity. In addition, implicated signaling pathways as mentioned above may also be analyzed by immunoblotting. Furthermore, we would also like to develop an *ex vivo* model of statin-induced myopathy. Single muscle fibers collected from the tibialis anterior of mice can be pretreated with LPS, followed by fluvastatin to measure atrogene expression. Importantly this model would afford the ability to investigate the contributing role of the NLRP3/caspase-1 inflammasome in a physiological system without the potential non-specific inhibitor effects. Fibers from $NLRP3^{-/-}$ mice or $caspase\text{-}1^{-/-}$ mice can both be used to further elucidate the statin myopathy signaling pathway.

Finally, it will be important to analyze samples from statin myopathy patients to determine the relevance of the NLRP3 inflammasome in human myopathies. Initial data generated by Dr. Jonathan Schertzer and Dr. Mark Tarnopolsky, provide enticing evidence from muscle biopsy samples of statin myopathy patients. NLRP3 gene expression is significantly higher in statin myopathy samples compared to control samples (Figure 15A). Moreover, higher caspase-1 activity was detected in the muscle of statin myopathy patients (Figure 15B).

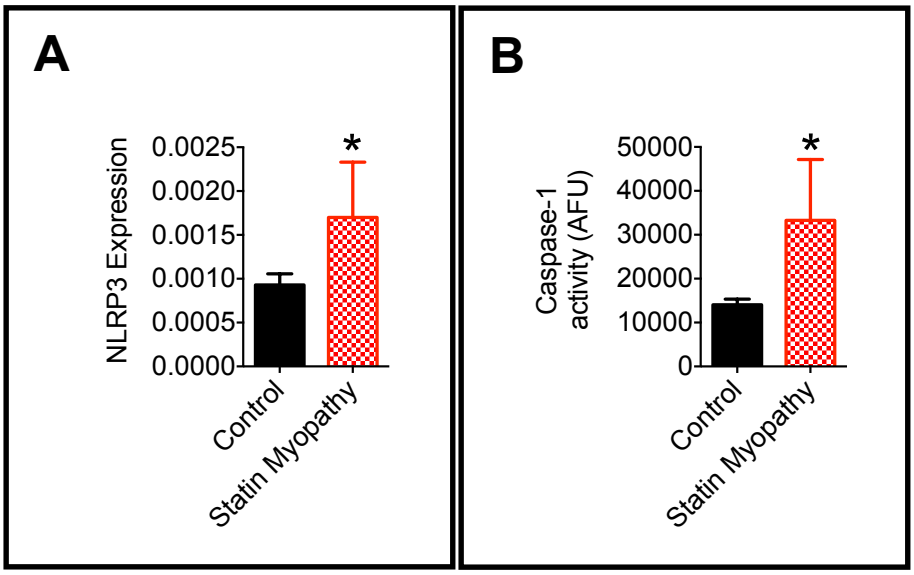

Figure 15| NLRP3/caspase-1 inflammasome activity and atrogene expression in statin myopathy patients.

Muscle biopsy samples from control and statin myopathy patients show elevated NLRP3 gene expression (A) and caspase-1 activity (B). Values are mean ± SD, n≥4 for all conditions, *significantly different from control patients by Student's T-Test.

6.0 CONCLUSION

The induction and progression of statin-induced myopathy is still not well understood, but the discovery of atrophy-related gene programs involved in statin myopathy will help in the discovery of new pathways implicated in this disease. Using an *in vitro* model, we presented work showing that the activation of caspase-1 through the NLRP3 inflammasome attenuates statin-induced myopathy as evidenced by the increased gene expression of key atrophy-related proteins at a lower dose of fluvastatin in primed C2C12 myotubes. This effect was found to be dependent on the isoprenoid depletion of GGPP, which was able to rescue atrogene induction by fluvastatin through restoration of FOXO3a phosphorylation. Future research will help to further elucidate the downstream effectors of the NLRP3 inflammasome that contribute to statin-induced myopathy. Ultimately, the novel finding of the involvement of this inflammatory pathway in statin-induced myopathy provides greater insight into proteins and pathways that can be targeted to generate new drug therapies for patients suffering from statin-induced myopathy.

7.0 REFERENCES

1. Endo, A., Kuroda, M. & Tsujita, Y. ML-236A, ML-236B, and ML-236C, new inhibitors of cholesterogenesis produced by *Penicillium citrinium*. *J. Antibiot. (Tokyo).* **29,** 1346–8 (1976).
2. Istvan, E. S. & Deisenhofer, J. Structural mechanism for statin inhibition of HMG-CoA reductase. *Science* **292,** 1160–4 (2001).
3. Jain, M. K. & Ridker, P. M. Anti-inflammatory effects of statins: clinical evidence and basic mechanisms. *Nat. Rev. Drug Discov.* **4,** 977–987 (2005).
4. Vrecer, M., Turk, S., Drinovec, J. & Mrhar, A. Use of statins in primary and secondary prevention of coronary heart disease and ischemic stroke. Meta-analysis of randomized trials. *Int. J. Clin. Pharmacol. Ther.* **41,** 567–77 (2003).
5. Maron, D. J., Fazio, S. & Linton, M. F. Current perspectives on statins. *Circulation* **101,** 207–213 (2000).
6. Goldstein, J. L. & Brown, M. S. Regulation of the mevalonate pathway. *Nature* **343,** 425–30 (1990).
7. Bellosta, S., Ferri, N., Bernini, F., Paoletti, R. & Corsini, A. Non-lipid-related effects of statins. *Ann. Med.* **32,** 164–76 (2000).
8. Taylor, F. *et al.* Statins for the primary prevention of cardiovascular disease. *Cochrane database Syst. Rev.* CD004816 (2013). doi:10.1002/14651858.CD004816.pub5
9. Buhaescu, I. & Izzedine, H. Mevalonate pathway: a review of clinical and therapeutical implications. *Clin. Biochem.* **40,** 575–584 (2007).
10. Henneman, L. *et al.* Detection of nonsterol isoprenoids by HPLC-MS/MS. *Anal. Biochem.* **383,** 18–24 (2008).
11. Konstantinopoulos, P. a, Karamouzis, M. V & Papavassiliou, A. G. Post-translational modifications and regulation of the RAS superfamily of GTPases as anticancer targets. *Nat. Rev. Drug Discov.* **6,** 541–555 (2007).
12. Takai, Y. *et al.* Small GTP-binding proteins. *Physiol. Rev.* **81,** 153–208 (2001).
13. Wong, W. W. L., Dimitroulakos, J., Minden, M. D. & Penn, L. Z. HMG-CoA reductase inhibitors and the malignant cell: the statin family of drugs as triggers of tumor-specific apoptosis. *Leukemia* **16,** 508–19 (2002).
14. Burda, P. & Aebi, M. The dolichol pathway of *N*-linked glycosylation. *Biochim. Biophys. Acta - Gen. Subj.* **1426,** 239–257 (1999).
15. Carlberg, M. *et al.* Mevalonic acid is limiting for *N*-linked glycosylation and translocation of the insulin-like growth factor-1 receptor to the cell surface:

evidence for a new link between 3-hydroxy-3-methylglutaryl-coenzyme A reductase and cell growth. *J. Biol. Chem.* **271,** 17453–17462 (1996).

16. Sacks, F. M. *et al.* The effect of pravastatin on coronary events after myocardial infarction in patients with average cholesterol levels. Cholesterol and Recurrent Events Trial investigators. *N. Engl. J. Med.* **335,** 1001–9 (1996).
17. Jacobs, D. *et al.* MRC/BHF Heart Protection Study of cholesterol lowering with simvastatin in 20 536 high-risk individuals: a randomised placebo controlled trial. *Lancet* **360,** 7–22 (2002).
18. Wenke, K. *et al.* Simvastatin reduces graft vessel disease and mortality after heart transplantation: a four-year randomized trial. *Circulation* **96,** 1398–402 (1997).
19. Blauw, G. J., Lagaay, A. M., Smelt, A. H. & Westendorp, R. G. Stroke, statins, and cholesterol: a meta-analysis of randomized, placebo-controlled, double-blind trials with HMG-CoA reductase inhibitors. *Stroke.* **28,** 946–50 (1997).
20. Davignon, J. Beneficial cardiovascular pleiotropic effects of statins. *Circulation* **109,** III-39–III-43 (2004).
21. Greenwood, J., Steinman, L. & Zamvil, S. S. Statin therapy and autoimmune disease: from protein prenylation to immunomodulation. *Nat. Rev. Immunol.* **6,** 358–70 (2006).
22. Rosenson, R. S., Tangney, C. C. & Casey, L. C. Inhibition of proinflammatory cytokine production by pravastatin. *Lancet* **353,** 983–984 (1999).
23. Massonnet, B. *et al.* Pharmacological inhibitors of the mevalonate pathway activate pro-IL-1 processing and IL-1 release by human monocytes. *Eur. Cytokine Netw.* **20,** 112–120 (2009).
24. Montero, M. T. *et al.* Hydroxymethylglutaryl-coenzyme A reductase inhibition stimulates caspase-1 activity and Th1-cytokine release in peripheral blood mononuclear cells. *Atherosclerosis* **153,** 303–313 (2000).
25. Liao, Y.-H. *et al.* HMG-CoA reductase inhibitors activate caspase-1 in human monocytes depending on ATP release and P2X7 activation. *J. Leukoc. Biol.* **93,** 289–299 (2013).
26. Frenkel, J. *et al.* Lack of isoprenoid products raises ex vivo interleukin-1β secretion in hyperimmunoglobulinemia D and periodic fever syndrome. *Arthritis Rheum.* **46,** 2794–2803 (2002).
27. Denes, A., Lopez-Castejon, G. & Brough, D. Caspase-1: is IL-1 just the tip of the ICEberg? *Cell Death Dis.* **3,** e338 (2012).
28. Sollberger, G., Strittmatter, G. E., Garstkiewicz, M., Sand, J. & Beer, H.-D. Caspase-1: the inflammasome and beyond. *Innate Immun.* **20,** 115–25 (2014).

29. Bergsbaken, T., Fink, S. L. & Cookson, B. T. Pyroptosis: host cell death and inflammation. *Nat. Rev. Microbiol.* **7,** 99–109 (2009).
30. Miao, E. A., Rajan, J. V. & Aderem, A. Caspase-1-induced pyroptotic cell death. *Immunol. Rev.* **243,** 206–214 (2011).
31. Thornberry, N. A. *et al.* Caspases: enemies within. *Science* **281,** 1312–6 (1998).
32. Timmer, J. C. & Salvesen, G. S. Caspase substrates. *Cell Death Differ.* **14,** 66–72 (2007).
33. Shen, J. *et al.* Caspase-1 recognizes extended cleavage sites in its natural substrates. *Atherosclerosis* **210,** 422–9 (2010).
34. Lüthi, A. U. & Martin, S. J. The CASBAH: a searchable database of caspase substrates. *Cell Death Differ.* **14,** 641–50 (2007).
35. Harvey, K. F. *et al.* Caspase-mediated cleavage of the ubiquitin-protein ligase Nedd4 during apoptosis. *J. Biol. Chem.* **273,** 13524–30 (1998).
36. Gu, Y., Sarnecki, C., Aldape, R. A., Livingston, D. J. & Su, M. S. Cleavage of poly(ADP-ribose) polymerase by interleukin-1 beta converting enzyme and its homologs TX and Nedd-2. *J. Biol. Chem.* **270,** 18715–8 (1995).
37. Kayalar, C., Ord, T., Testa, M. P., Zhong, L. T. & Bredesen, D. E. Cleavage of actin by interleukin 1 beta-converting enzyme to reverse DNase I inhibition. *Proc. Natl. Acad. Sci. U. S. A.* **93,** 2234–8 (1996).
38. Shao, W., Yeretssian, G., Doiron, K., Hussain, S. N. & Saleh, M. The caspase-1 digestome identifies the glycolysis pathway as a target during infection and septic shock. *J. Biol. Chem.* **282,** 36321–9 (2007).
39. Abderrazak, A. *et al.* NLRP3 inflammasome: from a danger signal sensor to a regulatory node of oxidative stress and inflammatory diseases. *Redox Biol.* **4,** 296–307 (2015).
40. Guo, H., Callaway, J. B. & Ting, J. P.-Y. Inflammasomes: mechanism of action, role in disease, and therapeutics. *Nat. Med.* **21,** 677–687 (2015).
41. Martinon, F. & Tschopp, J. Inflammatory caspases: linking an intracellular innate immune system to autoinflammatory diseases. *Cell* **117,** 561–574 (2004).
42. Schroder, K. & Tschopp, J. The inflammasomes. *Cell* **140,** 821–32 (2010).
43. Muñoz-Planillo, R. *et al.* K^+ efflux is the common trigger of NLRP3 inflammasome activation by bacterial toxins and particulate matter. *Immunity* **38,** 1142–1153 (2013).
44. Gross, O., Thomas, C. J., Guarda, G. & Tschopp, J. The inflammasome: an integrated view. *Immunol. Rev.* **243,** 136–51 (2011).
45. Sutterwala, F. S., Haasken, S. & Cassel, S. L. Mechanism of NLRP3 inflammasome

activation. *Ann. N. Y. Acad. Sci.* **1319,** 82–95 (2014).

46. Py, B. F., Kim, M.-S., Vakifahmetoglu-Norberg, H. & Yuan, J. Deubiquitination of NLRP3 by BRCC3 critically regulates inflammasome activity. *Molecular Cell* **49,** (2013).
47. Juliana, C. *et al.* Non-transcriptional priming and deubiquitination regulate NLRP3 inflammasome activation. *J. Biol. Chem.* **287,** 36617–22 (2012).
48. Stancu, C. & Sima, A. Statins: mechanism of action and effects. *J. Cell. Mol. Med.* **5,** 378–387 (2001).
49. Sathasivam, S. & Lecky, B. Statin induced myopathy. *BMJ* **337,** a2286 (2008).
50. Shah, R. V & Goldfine, A. B. Statins and risk of new-onset diabetes mellitus. *Circulation* **126,** e282–4 (2012).
51. Auer, J., Sinzinger, H., Franklin, B. & Berent, R. Muscle- and skeletal-related side-effects of statins: tip of the iceberg? *Eur. J. Prev. Cardiol.* **23,** 88–110 (2016).
52. Bruckert, E., Hayem, G., Dejager, S., Yau, C. & Bégaud, B. Mild to moderate muscular symptoms with high-dosage statin therapy in hyperlipidemic patients: the PRIMO study. *Cardiovasc. Drugs Ther.* **19,** 403–14 (2005).
53. Needham, M. & Mastaglia, F. L. Statin myotoxicity: a review of genetic susceptibility factors. *Neuromuscul. Disord.* **24,** 4–15 (2014).
54. Mishra, T. K. & Routray, S. Current perspectives on statins. *J. Indian Med. Assoc.* **101,** 381–383 (2003).
55. Pencina, M. J. *et al.* Application of new cholesterol guidelines to a population-based sample. *N. Engl. J. Med.* **370,** 1422–31 (2014).
56. Alfirevic, A. *et al.* Phenotype standardization for statin-induced myotoxicity. *Clin. Pharmacol. Ther.* **96,** 470–6 (2014).
57. Maghsoodi, N. & Wierzbicki, A. S. Statin myopathy: over-rated and under-treated. *Curr. Opin. Cardiol.* **31,** 417–425 (2016).
58. Dirks, A. J. & Jones, K. M. Statin-induced apoptosis and skeletal myopathy. *Am. J. Physiol. Cell Physiol.* **291,** C1208–12 (2006).
59. Thompson, P. D., Clarkson, P. & Karas, R. H. Statin-associated myopathy. *JAMA* **289,** 1681–90 (2003).
60. Tomaszewski, M., Stępień, K. M., Tomaszewska, J. & Czuczwar, S. J. Statin-induced myopathies. *Pharmacol. Rep.* **63,** 859–66 (2011).
61. Sirvent, P., Mercier, J. & Lacampagne, A. New insights into mechanisms of statin-associated myotoxicity. *Curr. Opin. Pharmacol.* **8,** 333–8 (2008).
62. De Pinieux, G. *et al.* Lipid-lowering drugs and mitochondrial function: effects of HMG-CoA reductase inhibitors on serum ubiquinone and blood lactate/pyruvate

ratio. *Br. J. Clin. Pharmacol.* **42,** 333–7 (1996).

63. Päivä, H. *et al.* High-dose statins and skeletal muscle metabolism in humans: a randomized, controlled trial. *Clin. Pharmacol. Ther.* **78,** 60–8 (2005).
64. Noh, Y. H. *et al.* Inhibition of oxidative stress by coenzyme Q10 increases mitochondrial mass and improves bioenergetic function in optic nerve head astrocytes. *Cell Death Dis.* **4,** e820 (2013).
65. Deichmann, R., Lavie, C. & Andrews, S. Coenzyme q10 and statin-induced mitochondrial dysfunction. *Ochsner J.* **10,** 16–21 (2010).
66. Sirvent, P., Mercier, J., Vassort, G. & Lacampagne, A. Simvastatin triggers mitochondria-induced Ca^{2+} signaling alteration in skeletal muscle. *Biochem. Biophys. Res. Commun.* **329,** 1067–1075 (2005).
67. Sack, M. N. *et al.* Mitochondrial depolarization and the role of uncoupling proteins in ischemia tolerance. *Cardiovasc. Res.* **72,** 210–9 (2006).
68. Liantonio, A. *et al.* Fluvastatin and atorvastatin affect calcium homeostasis of rat skeletal muscle fibers in vivo and in vitro by impairing the sarcoplasmic reticulum/mitochondria Ca^{2+}-release system. *J. Pharmacol. Exp. Ther.* **321,** 626–34 (2007).
69. Pinton, P., Giorgi, C., Siviero, R., Zecchini, E. & Rizzuto, R. Calcium and apoptosis: ER-mitochondria Ca^{2+} transfer in the control of apoptosis. *Oncogene* **27,** 6407–18 (2008).
70. Kwak, H.-B. *et al.* Simvastatin impairs ADP-stimulated respiration and increases mitochondrial oxidative stress in primary human skeletal myotubes. *Free Radic. Biol. Med.* **52,** 198–207 (2012).
71. Johnson, T. E. *et al.* Statins induce apoptosis in rat and human myotube cultures by inhibiting protein geranylgeranylation but not ubiquinone. *Toxicol. Appl. Pharmacol.* **200,** 237–250 (2004).
72. Sacher, J., Weigl, L., Werner, M., Szegedi, C. & Hohenegger, M. Delineation of myotoxicity induced by 3-Hydroxy-3-methylglutaryl CoA reductase inhibitors in human skeletal muscle cells. *J. Pharmacol. Exp. Ther.* **314,** 1032–1041 (2005).
73. Apostolopoulou, M., Corsini, A. & Roden, M. The role of mitochondria in statin-induced myopathy. *Eur. J. Clin. Invest.* **45,** 745–54 (2015).
74. Egerman, M. A. & Glass, D. J. Signaling pathways controlling skeletal muscle mass. *Crit. Rev. Biochem. Mol. Biol.* **49,** 59–68 (2014).
75. Hirata, A. *et al.* Expression profiling of cytokines and related genes in regenerating skeletal muscle after cardiotoxin injection: a role for osteopontin. *Am. J. Pathol.* **163,** 203–15 (2003).

76. Florini, J. R., Ewton, D. Z. & Coolican, S. A. Growth hormone and the insulin-like growth factor system in myogenesis. *Endocr. Rev.* **17,** 481–517 (1996).
77. Engert, J. C., Berglund, E. B. & Rosenthal, N. Proliferation precedes differentiation in IGF-1-stimulated myogenesis. *J. Cell Biol.* **135,** 431–40 (1996).
78. Schiaffino, S. & Mammucari, C. Regulation of skeletal muscle growth by the IGF1-Akt/PKB pathway: insights from genetic models. *Skelet. Muscle* **1,** 4 (2011).
79. Mullen, P. J. *et al.* Susceptibility to simvastatin-induced toxicity is partly determined by mitochondrial respiration and phosphorylation state of Akt. *Biochim. Biophys. Acta* **1813,** 2079–87 (2011).
80. Lecker, S. H., Solomon, V., Mitch, W. E. & Goldberg, A. L. Muscle protein breakdown and the critical role of the ubiquitin-proteasome pathway in normal and disease states. *J. Nutr.* **129,** 227S–237S (1999).
81. Glickman, M. H. *et al.* The ubiquitin-proteasome proteolytic pathway: destruction for the sake of construction. *Physiol. Rev.* **82,** 373–428 (2002).
82. Baumeister, W., Walz, J., Zühl, F. & Seemüller, E. The proteasome: paradigm of a self-compartmentalizing protease. *Cell* **92,** 367–380 (1998).
83. Lecker, S. H. Ubiquitin-protein ligases in muscle wasting: multiple parallel pathways? *Curr. Opin. Clin. Nutr. Metab. Care* **6,** 271–5 (2003).
84. McElhinny, A. S., Kakinuma, K., Sorimachi, H., Labeit, S. & Gregorio, C. C. Muscle-specific RING finger-1 interacts with titin to regulate sarcomeric M-line and thick filament structure and may have nuclear functions via its interaction with glucocorticoid modulatory element binding protein-1. *J. Cell Biol.* **157,** 125–36 (2002).
85. Pizon, V. *et al.* Transient association of titin and myosin with microtubules in nascent myofibrils directed by the MURF2 RING-finger protein. *J. Cell Sci.* **115,** 4469–82 (2002).
86. Chen, Y.-W. *et al.* Early onset of inflammation and later involvement of TGF in Duchenne muscular dystrophy. *Neurology* **65,** 826–834 (2005).
87. Mallinson, J. E., Constantin-Teodosiu, D., Sidaway, J., Westwood, F. R. & Greenhaff, P. L. Blunted Akt/FOXO signalling and activation of genes controlling atrophy and fuel use in statin myopathy. *J. Physiol.* **587,** 219–30 (2009).
88. Hanai, J. *et al.* The muscle-specific ubiquitin ligase atrogin-1/MAFbx mediates statin-induced muscle toxicity. *J. Clin. Invest.* **117,** 3940–51 (2007).
89. Cao, P. *et al.* Statin-induced muscle damage and atrogin-1 induction is the result of a geranylgeranylation defect. *FASEB J.* **23,** 2844–54 (2009).
90. Sandri, M. *et al.* Foxo transcription factors induce the atrophy-related ubiquitin

ligase atrogin-1 and cause skeletal muscle atrophy. *Cell* **117,** 399–412 (2004).

91. Lee, S. W. *et al.* Regulation of muscle protein degradation: coordinated control of apoptotic and ubiquitin-proteasome systems by phosphatidylinositol 3 kinase. *J. Am. Soc. Nephrol.* **15,** 1537–45 (2004).
92. Stitt, T. N. *et al.* The IGF-1/PI3K/Akt Pathway Prevents Expression of Muscle Atrophy-Induced Ubiquitin Ligases by Inhibiting FOXO Transcription Factors. *Mol. Cell* **14,** 395–403 (2004).
93. Sandri, M. Signaling in muscle atrophy and hypertrophy. *Physiology (Bethesda).* **23,** 160–70 (2008).
94. Kamei, Y. *et al.* Skeletal muscle FOXO1 (FKHR) transgenic mice have less skeletal muscle mass, down-regulated Type I (slow twitch/red muscle) fiber genes, and impaired glycemic control. *J. Biol. Chem.* **279,** 41114–23 (2004).
95. Liu, C.-M. *et al.* Effect of RNA oligonucleotide targeting Foxo-1 on muscle growth in normal and cancer cachexia mice. *Cancer Gene Ther.* **14,** 945–52 (2007).
96. Cai, D. *et al.* IKKβ/NF-κB activation causes severe muscle wasting in mice. *Cell* **119,** 285–298 (2004).
97. Li, W. *et al.* Interleukin-1 stimulates catabolism in C2C12 myotubes. *Am. J. Physiol. Cell Physiol.* **297,** C706–14 (2009).
98. Henriksbo, B. D. *et al.* Fluvastatin causes NLRP3 inflammasome-mediated adipose insulin resistance. *Diabetes* **63,** 3742–7 (2014).
99. Bauernfeind, F. G. *et al.* Cutting edge: NF-kappaB activating pattern recognition and cytokine receptors license NLRP3 inflammasome activation by regulating NLRP3 expression. *J. Immunol.* **183,** 787–91 (2009).
100. Zhao, J. *et al.* FoxO3 coordinately activates protein degradation by the autophagic/lysosomal and proteasomal pathways in atrophying muscle cells. *Cell Metab.* **6,** 472–83 (2007).
101. Greer, E. L. & Brunet, A. FOXO transcription factors at the interface between longevity and tumor suppression. *Oncogene* **24,** 7410–7425 (2005).
102. Zhang, X., Tang, N., Hadden, T. J. & Rishi, A. K. Akt, FoxO and regulation of apoptosis. *Biochim. Biophys. Acta - Mol. Cell Res.* **1813,** 1978–1986 (2011).
103. Sacheck, J. M., Ohtsuka, A., McLary, S. C. & Goldberg, A. L. IGF-1 stimulates muscle growth by suppressing protein breakdown and expression of atrophy-related ubiquitin ligases, atrogin-1 and MuRF1. *Am. J. Physiol. Endocrinol. Metab.* **287,** E591–601 (2004).
104. Larsen, S. *et al.* Simvastatin effects on skeletal muscle: relation to decreased mitochondrial function and glucose intolerance. *J. Am. Coll. Cardiol.* **61,** 44–53

(2013).
105. Beth A. Parker, P. D. T. Effect of statins on skeletal muscle: exercise, myopathy, and muscle outcomes. *Exerc. Sport Sci. Rev.* **40,** 188 (2012).
106. Bonifacio, A., Sanvee, G. M., Bouitbir, J. & Krähenbühl, S. The AKT/mTOR signaling pathway plays a key role in statin-induced myotoxicity. *Biochim. Biophys. Acta - Mol. Cell Res.* **1853,** 1841–1849 (2015).
107. Wagner, B. K. *et al.* A small-molecule screening strategy to identify suppressors of statin myopathy. (2011).
108. Goodman, C. A. *et al.* Statin-induced increases in atrophy gene expression occur independently of changes in PGC1α protein and mitochondrial content. *PLoS One* **10,** e0128398 (2015).
109. Gazzerro, P. *et al.* Pharmacological actions of statins: a critical appraisal in the management of cancer. *Pharmacol. Rev.* **64,** 102–146 (2012).
110. Sakamoto, K., Mikami, H. & Kimura, J. Involvement of organic anion transporting polypeptides in the toxicity of hydrophilic pravastatin and lipophilic fluvastatin in rat skeletal myofibres. *Br. J. Pharmacol.* **154,** 1482–90 (2008).
111. Taha, D. A. *et al.* The role of acid-base imbalance in statin-induced myotoxicity. *Transl. Res.* **174,** 140–160.e14 (2016).
112. Bitzur, R., Cohen, H., Kamari, Y. & Harats, D. Intolerance to statins: mechanisms and management. doi:10.2337/dcS13-2038
113. Netea, M. G. *et al.* Differential requirement for the activation of the inflammasome for processing and release of IL-1beta in monocytes and macrophages. *Blood* **113,** 2324–35 (2009).
114. Gaidt, M. M. *et al.* Human monocytes engage an alternative inflammasome pathway. *Immunity* **44,** 833–46 (2016).
115. Kuijk, L. M. *et al.* Statin synergizes with LPS to induce IL-1β release by THP-1 cells through activation of caspase-1. *Mol. Immunol.* **45,** 2158–2165 (2008).
116. Lecker, S. H. *et al.* Multiple types of skeletal muscle atrophy involve a common program of changes in gene expression. *FASEB J.* **18,** 39–51 (2004).
117. Kuijk, L. M. *et al.* HMG-CoA reductase inhibition induces IL-1beta release through Rac1/PI3K/PKB-dependent caspase-1 activation. *Blood* **112,** 3563–73 (2008).
118. Montero, M. T., Matilla, J., Gomez-Mampaso, E. & Lasuncion, M. A. Geranylgeraniol regulates negatively caspase-1 autoprocessing: implication in the Th1 response against *Mycobacterium tuberculosis*. *J. Immunol.* **173,** 4936–4944 (2004).
119. Reboldi, A. *et al.* Inflammation: 25-Hydroxycholesterol suppresses interleukin-1-

driven inflammation downstream of type I interferon. *Science* **345,** 679–84 (2014).
120. Gold, E. S. *et al.* 25-Hydroxycholesterol acts as an amplifier of inflammatory signaling. *Proc. Natl. Acad. Sci. U. S. A.* **111,** 10666–71 (2014).
121. Siddle, K. Signalling by insulin and IGF receptors: supporting acts and new players. *J. Mol. Endocrinol.* **47,** R1–R10 (2011).
122. Hemmings, B. A. & Restuccia, D. F. PI3K-PKB/Akt pathway. *Cold Spring Harb. Perspect. Biol.* **4,** a011189–a011189 (2012).
123. Guertin, D. A. *et al.* Ablation in mice of the mTORC components raptor, rictor, or mLST8 reveals that mTORC2 is required for signaling to Akt-FOXO and PKCalpha, but not S6K1. *Dev. Cell* **11,** 859–71 (2006).
124. Ogura, T. *et al.* Simvastatin reduces insulin-like growth factor-1 signaling in differentiating C2C12 mouse myoblast cells in an HMG-CoA reductase inhibition-independent manner. *J. Toxicol. Sci.* **32,** 57–67 (2007).
125. Opal, S. M. *et al.* Relationship between plasma levels of lipopolysaccharide (LPS) and LPS-binding protein in patients with severe sepsis and septic shock. *J. Infect. Dis.* **180,** 1584–9 (1999).
126. Guo, Y. *et al.* Serum levels of lipopolysaccharide and 1,3-β-D-Glucan refer to the severity in patients with Crohn's disease. *Mediators Inflamm.* **2015,** 1–9 (2015).
127. Ghonime, M. G. *et al.* Inflammasome priming by lipopolysaccharide is dependent upon ERK signaling and proteasome function. *J. Immunol.* **192,** 3881–8 (2014).
128. Le Feuvre, R. A., Brough, D., Iwakura, Y., Takeda, K. & Rothwell, N. J. Priming of macrophages with lipopolysaccharide potentiates P2X7-mediated cell death via a caspase-1-dependent mechanism, independently of cytokine production. *J. Biol. Chem.* **277,** 3210–3218 (2002).
129. Franchi, L., Muñoz-Planillo, R. & Núñez, G. Sensing and reacting to microbes through the inflammasomes. *Nat. Immunol.* **13,** 325–32 (2012).
130. Li, X. *et al.* MicroRNA-30d regulates cardiomyocyte pyroptosis by directly targeting foxo3a in diabetic cardiomyopathy. *Cell Death Dis.* **5,** e1479 (2014).
131. Horsley, V., Jansen, K. M., Mills, S. T. & Pavlath, G. K. IL-4 acts as a myoblast recruitment factor during mammalian muscle growth. *Cell* **113,** 483–494 (2003).
132. Miao, E. A., Rajan, J. V & Aderem, A. Caspase-1-induced pyroptotic cell death. *Immunol. Rev.* **243,** 206–14 (2011).